Zeitschrift: Eclogae Geologicae Helvetiae
Herausgeber: Schweizerische Geologische Gesellschaft
Band: 75 (1982)
Heft: 1

Artikel: Magnetic properties of deformed oolitic limestones from the Swiss Alps : the correlation of magnetic anisotropy and strain

Autor: Kligfield, Roy / Lowrie, William / Pfiffner, O. Adrian

DOI: https://doi.org/10.5169/seals-165221

Eclogae geol. Helv.	Vol. 75/1	Pages 127-157	17 figures in the text and 2 tables	Basle, March 1982

Magnetic properties of deformed oolitic limestones from the Swiss Alps: the correlation of magnetic anisotropy and strain

By ROY KLIGFIELD[1])[3]), WILLIAM LOWRIE[1]) and O. ADRIAN PFIFFNER[2])

ABSTRACT

Deformed Jurassic oolitic limestones from the sedimentary cover of the Aar massif (Swiss Alps) contain abundant magnetite and hematite. The magnetic properties of the limestones were studied in order to compare quantitatively the magnetic susceptibility anisotropy with the finite strain in the rocks. Laboratory investigations included alternating field and thermal demagnetization, acquisition of isothermal remanent magnetization, low temperature studies, high field torque-meter measurements, rotational hysteresis studies, thin and polished section examination, and measurement of the low-field magnetic susceptibility anisotropy. Ooids within undeformed oolites show a concentric structure which is usually preserved in deformed oolites. During metamorphism as well as laboratory heating chamosite decomposed at temperatures above 400 °C to form magnetite. Newly crystallized magnetites have euhedral individual grain shapes but their overall distribution is controlled by the original concentric structure. The resultant stringing together of magnetites gives rise to a mimetic shape anisotropy directly related to the shapes of the deformed ooids. In hematite-rich layers the preferred orientation of hematite basal planes about the deformed ooids gives rise to a crystallographically controlled anisotropy of magnetic susceptibility.

The principal susceptibility axes ($k_{max} > k_{int} > k_{min}$) of samples at each site are tightly grouped. k_{min} axes are perpendicular to the cleavage and to the XY planes of the strain ellipsoid ($X > Y > Z$). k_{max} axes are parallel to the maximum extension (X) and k_{int} axes are usually parallel to the regional strike. A quantitative correlation has been established between the finite strains determined from the ooids and the magnetic susceptibility anisotropy in the hematite layers. The results demonstrate that it is possible to obtain strain results rapidly using magnetic susceptibility data in these rocks.

ZUSAMMENFASSUNG

Deformierte oolithische Kalke jurassischen Alters aus der Sedimenthülle des Aarmassivs (Zentralalpen) enthalten reichlich Magnetit und Hämatit. Um die Anisotropie der magnetischen Suszeptibilität quantitativ mit dem Verformungszustand der Gesteine zu vergleichen, wurden die magnetischen Eigenschaften dieser Gesteine untersucht. Folgende Untersuchungen wurden im Labor durchgeführt: Wechselfeld- und thermische Entmagnetisierungen, isothermische remanente Magnetisierung, Tieftemperatur-Experimente, Messungen des Drehmoments sowie der Rotationshysterese in hohen Feldern und Messungen der Anisotropie der magnetischen Suszeptibilität. Ooide undeformierter Oolithe besitzen

[1]) Institut für Geophysik, ETH-Hönggerberg, CH-8093 Zürich, Switzerland.

[2]) Institut de Géologie, 11, rue Emile-Argand, Université de Neuchâtel, CH-2000 Neuchâtel, Switzerland.

[3]) New address: Department of Geological Sciences, University of Colorado, Boulder, Colorado 80309, USA.

eine konzentrische Struktur, die bei deformierten Oolithen im allgemeinen erhalten blieb. Während der Metamorphose sowie bei Laborversuchen über 400 °C bildet sich aus Chamosit Magnetit. Diese Neubildungen sind euhedral, aber ihre Verteilung widerspiegelt die ursprünglich konzentrische Struktur der Ooide. Diese mimetische Textur ergibt eine magnetische Anisotropie, welche direkt von der Form der Ooide abhängig ist. In hämatitreichen Oolithen verursacht die bevorzugte Einregelung der Basisfläche der Hämatitplättchen eine kristallographisch kontrollierte magnetische Anisotropie.

An jedem einzelnen untersuchten Aufschluss sind die Hauptachsen der Suszeptibilität ($k_{max} > k_{int} > k_{min}$) aller Proben sehr gleichmässig orientiert. Die k_{min}-Achsen sind senkrecht sowohl zur Schieferung als auch zur Plättungsebene des Verformungsellipsoides ($X > Y > Z$). Die k_{max}-Achsen sind parallel zur Streckungsrichtung (X), und die k_{int}-Achsen sind parallel zum allgemeinen Streichen. Für hämatitreiche Oolithe besteht eine quantitative Korrelation zwischen dem Verformungszustand, der aufgrund der Ooide ermittelt wurde, und der Anisotropie der magnetischen Suszeptibilität. Die Ergebnisse zeigen, dass die magnetische Suszeptibilität es in dieser Gesteinsart erlaubt, sehr rasch den Verformungszustand zu bestimmen.

RÉSUMÉ

Les calcaires oolitiques déformés du Jurassique de la couverture sédimentaire du massif de l'Aar (Alpes suisses) sont riches en magnétite et hématite. Les propriétés magnétiques ont été étudiées pour comparer d'une manière quantitative l'anisotropie de la susceptibilité magnétique au taux de la déformation subi des roches. Les études suivantes ont été effectués au laboratoire: désaimantation thermique et en champs alternants, acquisition de l'aimantation remanente isothermale, essais à basses températures, mesures du couple de torsion ainsi que de l'hystérèse rotationnelle en champ haut, études des lames minces et surfaces polies, et analyse de l'anisotropie de la susceptibilité magnétique. Dans les oolites non-déformées les ooïdes montrent une structure concentrique qui est en général préservée après une déformation. Pendant le métamorphisme, ainsi qu'après le chauffage en laboratoire à des températures dépassant 400 °C, la chamosite se décompose pour former de la magnétite. Ces magnétites sont euhédrales, mais leur répartition est contrôlée par la structure concentrique primordiale. Cette texture mimétique est directement reliée à la forme des ooïdes déformés. Dans les oolites riches en hématite l'orientation préférentielle du plan basal des plaquettes d'hématite donne naissance à une anisotropie magnétique contrôlée par la cristallographie.

Pour chacun des affleurements étudiés les axes principaux de la susceptibilité magnétique ($k_{max} > k_{int} > k_{min}$) des échantillons se groupent bien autour d'un maximum. Les axes k_{min} sont perpendiculaires au clivage et au plan d'aplatissement de l'ellipsoide de déformation ($X > Y > Z$). Les axes k_{max} sont parallèles à l'élongation (X) et les axes k_{int} sont parallèles à la direction générale des structures. Dans le cas des oolites riches en hématite il existe une corrélation quantitative entre le taux de la déformation, déterminé à la base des ooïdes, et l'anisotropie de la susceptibilité magnétique. Les résultats montrent qu'il est possible de déterminer les taux de la déformation dans ce type de roches d'une manière très rapide à l'aide de l'anisotropie de la susceptibilité magnétique.

Introduction

Of great importance to structural geologists is the ability to determine quantitatively the shape changes which occur in rocks due to deformation processes. ALBERT HEIM (1878) was one of the first to appreciate the significance of deformed ooids and fossils and to note the possibility of using the shapes of these objects to determine the finite strain in rocks. It was not until the classic work of CLOOS (1947) on the South Mountain fold that a rigorous approach was made to the study of systematic changes in finite strain using deformed oolites. Since that time much modern work has evolved which enables finite strain to be evaluated from deformed oolites (RAMSAY 1967, DUNNET 1969). One of the serious disadvantages of these methods is that the detailed field, laboratory and mathematical analyses necessary are very time consuming. Recently it has been shown that in certain instances estimates of

finite strain can be made very rapidly from magnetic susceptibility measurements (RATHORE 1979, KLIGFIELD et al. 1981). It is of practical interest to use this method in suitable rock types to obtain a very large density of strain measurements in a reasonably short period of time.

A thin, ferruginous oolitic limestone outcrops throughout much of the Helvetic zone of Switzerland (Fig. 1), a classic region of Alpine basement cover tectonics. Already in 1919, HEIM noted both the presence of magnetites in this oolite and the possibility of determining the strain suffered by the rocks on the basis of the shape of the ooids. BAKER (1964) discovered a correspondence between the magnetic susceptibility anisotropy and the finite strain axes in this oolite in the Maderanertal region. The present work reinvestigates this result in more detail at several localities. In particular we investigate the quantitative correlation of finite strain and magnetic susceptibility anisotropy with the goal of determining strain independently from measurements of the magnetic properties alone.

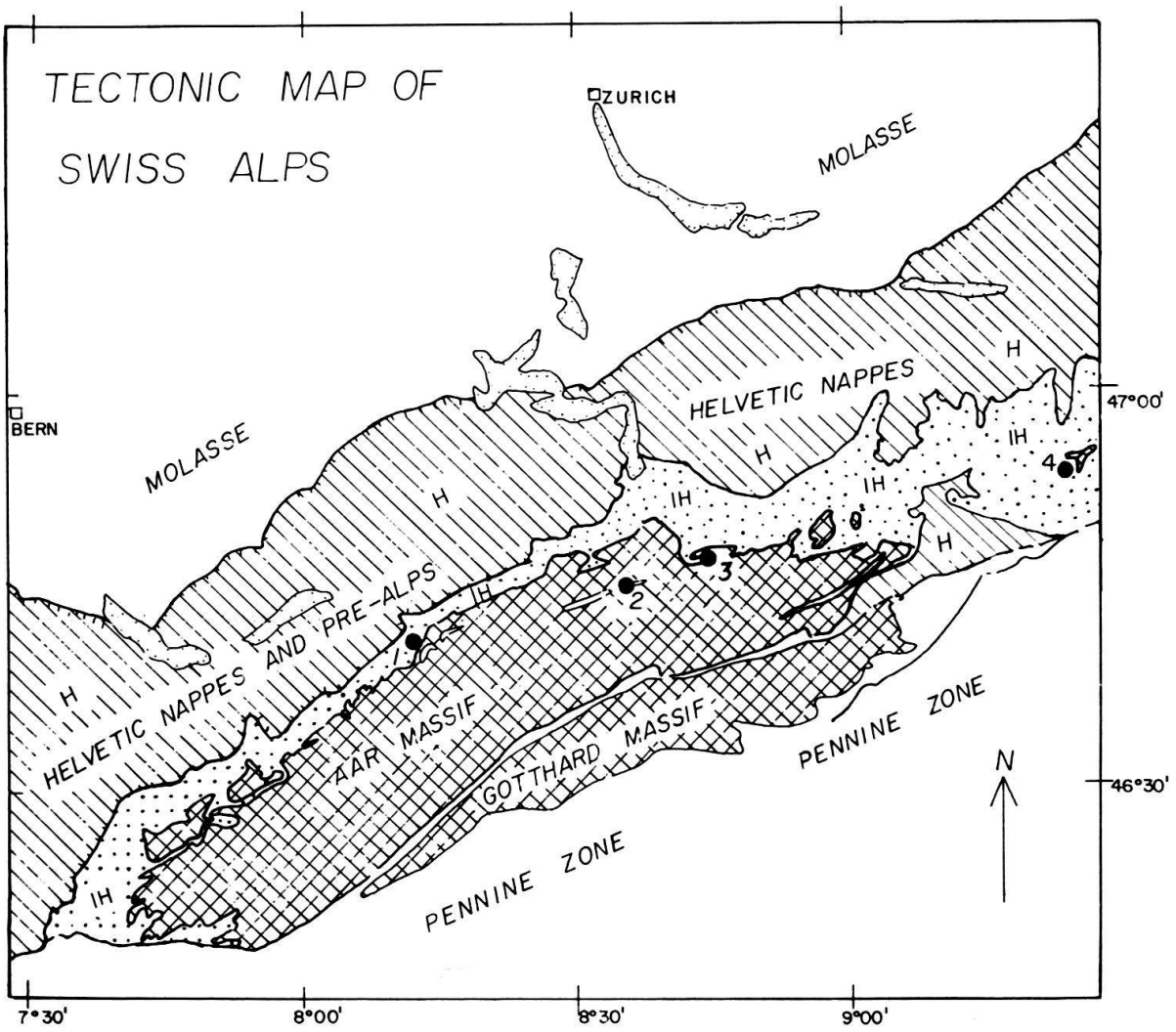

Fig. 1. Tectonic sketch map of Swiss Alps showing site localities. Numbered sites as follows: 1: Urbachtal, 2: Färnigen, 3: Maderanertal, 4: Vättis. Key to symbols: H: Helvetic nappes and overlying Penninic Klippe (e.g. Prealps), IH: Infrahelvetic complex (autochthonous and para-autochthonous cover of the Aar massif, allochthonous and exotic units).

Geological background

Samples were collected in central and eastern Switzerland at the following localities (Fig. 1): 1: Urbachtal, 2: Färnigen, 3: Maderanertal, 4: Vättis. Samples were drilled in the field from folds at Maderanertal. Oriented block samples were collected from folds at Vättis, Urbachtal and Färnigen and were drilled out in the laboratory.

The rocks investigated occur as a thin (0.1–5 m) layer of Middle Jurassic age. They are matrix supported oolitic limestones. The matrix consists mainly of micritic calcite whose grain size increases from 3 to 10 μm with increasing state of deformation (PFIFFNER 1981a). The ooids on the other hand consist of chamosite (or chamosite and siderite), hematite, magnetite, pyrite and on occasion ankerite–dolomite.

Two types of oolitic limestones can be distinguished in outcrop (Fig. 2) and in thin section (Fig. 3). *Type I* is a dark red to black colored, reddish-weathering oolite which contains only hematite as ferromagnetic mineral; *Type II* is a green colored chamosite oolite, weathering to yellow, and contains both magnetite and hematite. Accessory sulfides also occur and include pyrite, marcasite and sometimes pyrrhotite (DÉVERIN 1945).

The oolite occurs 10–100 m above the base of the sedimentary cover of the Aar massif. Its exact age is Upper Bajocian–Lower Callovian (DOLLFUS 1965). The sediments which overlie it in a sharp, concordant stratigraphic contact are of Middle Oxfordian (Argovian) age and consist of micritic limestones. The stratigraphic gap

Fig. 2. Field appearance of ferruginous iron oolite. a: Characteristic banding on weathered surface at Maderanertal site, showing alteration of dark, hematite-rich layers (Type I) with yellow weathering magnetite-rich layers (Type II). b: Syncline at Vättis.

between the two includes at least the *Quenstedtoceras mariae* and *Cardioceras cordatum* zones, and together with the occurrence of a pelagic fauna (e.g. cephalopods) within both the oolite and the overlying limestone, suggests subsidence (rather than uplift and emersion) during and after the sedimentation of the oolite.

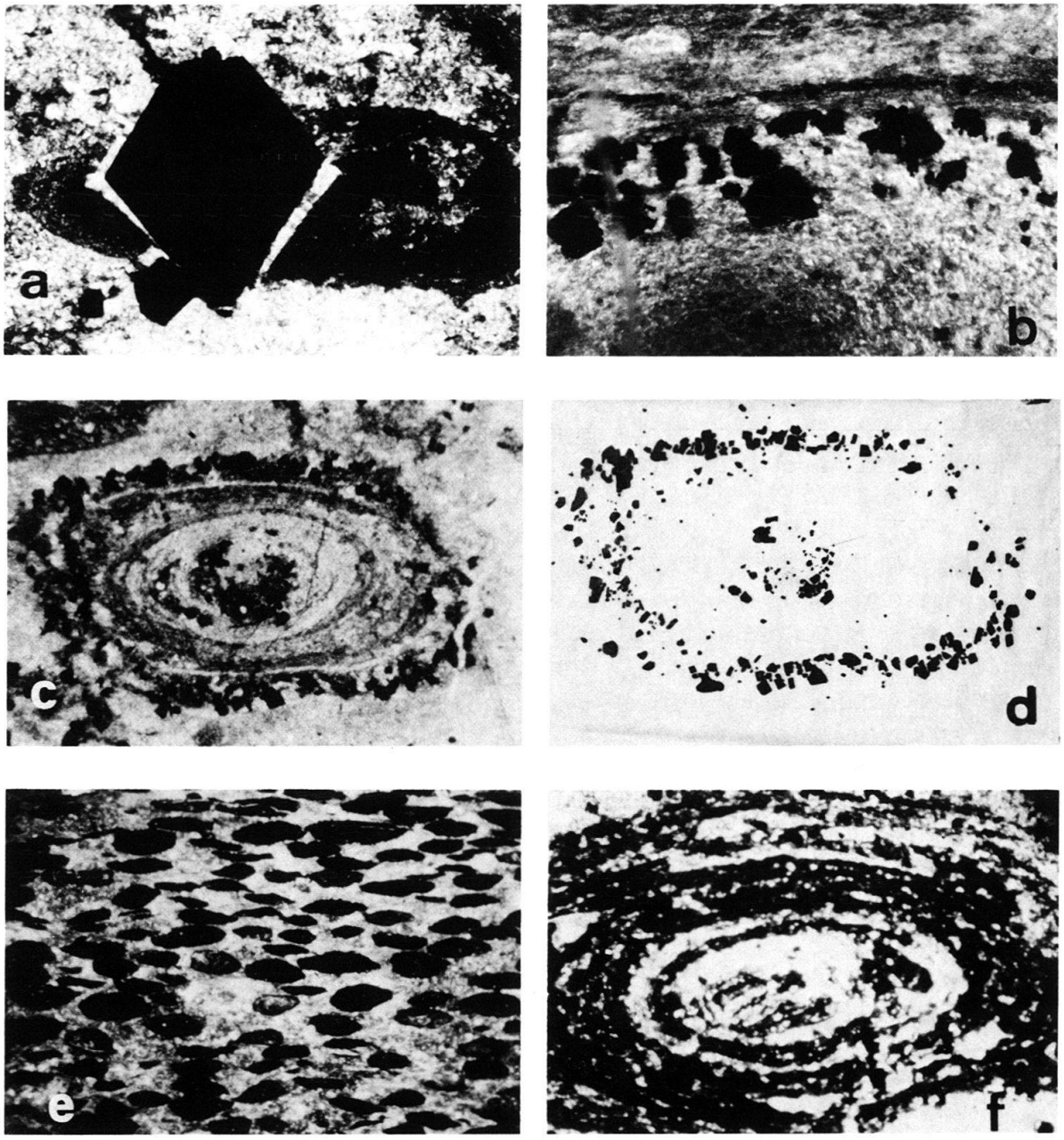

Fig. 3. Photomicrographs showing mimetic fabrics of oolitic limestones. a: Magnetite overgrowth on chamosite ooid. The magnetite crystallized before the last increment of deformation. Pressure solved quartz grew as fibres in extension direction. Width of field of view is 0.68 mm. b: Stringing together of euhedral magnetites along curved ooid boundary. Width of field of view 0.55 mm, Urbachtal. c: Euhedral magnetites rimming chamosite ooid. Width of field of view 2.19 mm. Photograph taken using combination of reflected and transmitted light on infrared film. d: Tracing of individual magnetites of Figure 3c showing their overall elliptical distribution. e: Magnetite-rich oolite, Urbachtal. The ooids have been completely replaced by fine-grained magnetite. Width of field of view 8.75 mm. f: Hematite ooid showing ellipsoidal distribution of hematite grains, Urbachtal. Width of field of view is 0.88 mm.

There are three possible sources of iron for the formation of ferruginous oolites (FÜCHTBAUER & MÜLLER 1970, p. 525 ff.): a) reaction of iron-rich minerals with seawater at the subsurface; b) volcanic/magmatic activity; and c) alteration of the rocks on an emerged land mass. The first of these mechanisms can only account for local ferruginous formation and a volcanic land mass is not known to have occurred. This leaves an emerged land mass as the most likely source. As DOLLFUS (1965) noted, the thickness of the oolite decreases from the originally northern domains (Aar massif cover) towards the more southerly ones (Helvetic nappes); moreover an emerged land mass (the Bohemian massif) was situated to the northeast.

KIMBERLEY (1979) suggested a mode of ferruginous oolite formation by which an oolite containing calcareous ooids was covered by an ordinary mud rich in organic matter; subsequent leaching of iron would then lead to the ferruginization of the underlying oolite. BRADSHAW et al. (1979) criticized this replacement model on petrographic and stratigraphic grounds. In particular, it does not explain the relatively highly ellipsoidal, uniformly oriented, concentric chamosite ooids occurring in a matrix-supported oolite encountered in our area.

Although several phases of deformation can be recognized in these regions (MILNES & PFIFFNER 1977, 1980, PFIFFNER 1977, 1978, SPÖRLI 1966, BRÜCKNER 1943), not all of them resulted in penetrative deformation. In general a major schistosity-forming phase (known locally at localities 3 and 4 as the "Calanda" phase) is followed by a nonpenetrative crenulating phase (known as the "Ruchi" phase). The structural settings of the folds sampled in the four areas are shown in the schematic cross sections of Figure 4.

At Vättis a metamorphic event reaching greenschist facies is believed to have occurred after the Calanda phase (PFIFFNER 1977, 1981b). In localities 2, 3 and 4 temperatures attained during this metamorphism were of the order of 350–400 °C (FREY 1978) and were slightly lower at locality 1. The metamorphic event led to the formation of siderite and magnetite in the oolites. Siderite occurs within chamosite ooids in a patchy fashion, but never disturbs the ellipsoidal shape of the ooids. The ellipticity of the ooids does not depend on the volume percent (5–95%) of siderite present (PFIFFNER 1977). If siderite had grown during diagenesis one would expect to see such a dependence as well as a viscosity contrast between chamosite and siderite (irregular shape of some of the ooids) and deformed patches of siderite. None of these features have been observed.

The presence of magnetite grains as perfectly euhedral crystals without any trace of deformation (Fig. 3a), the general lack of pressure shadows, and the fact that the magnetites grew over the already deformed ooids all indicate that the magnetites crystallized after the deformation (HEIM 1919; DEVERIN 1945). The cleavage traces are never found to bend around the magnetites as would be expected if they had grown before deformation (e.g. in a diagenetic process). However, upon closer examination it is possible to observe pressure shadows around the ends of some of the magnetite crystals (Fig. 3a). They consist of infilled fibrous vein material which serves as indicator of the incremental extension direction of the deformation in the rock (DURNEY & RAMSAY 1973). Although the individual magnetites cut the walls of deformed ooids, the presence of the fibrous calcite within the pressure shadows indicates that deformation was still occurring during the magnetite crystallization.

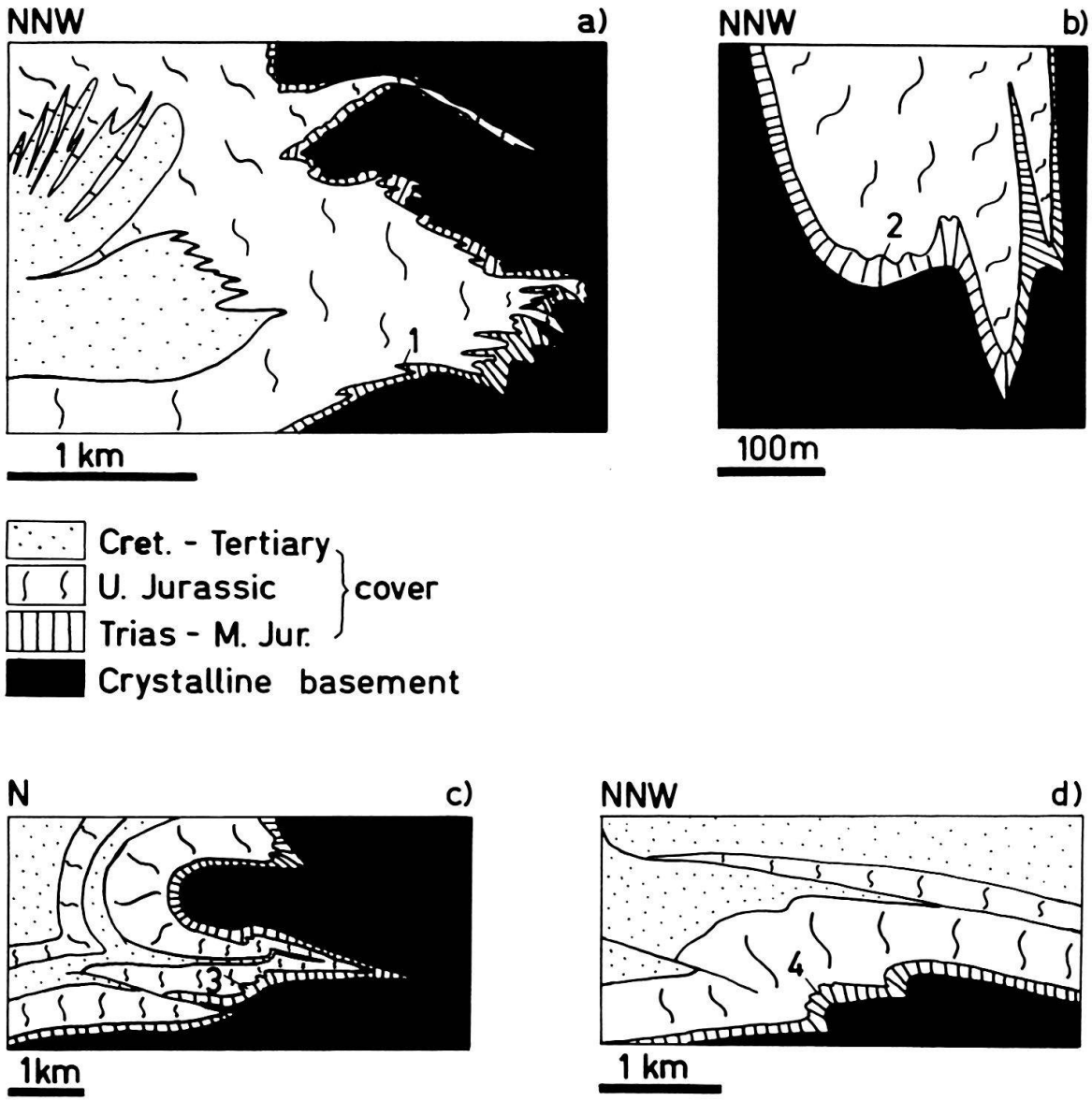

Fig. 4. Cross sections showing structural setting of folds sampled. a: Urbachtal after MÜLLER (1938); b: Färnigen after HEIM & HEIM (1916); c: Maderanertal after BRÜCKNER (1943) and TAN (1976); d: Vättis after PFIFFNER (1980).

Hence these magnetites were crystallized near the end of the deformation which produced the elliptical ooid shapes in thin section. The amount of fibrous vein material preserved in the pressure shadows about the magnetites reveals the last incremental stages of this deformation. It is at present not possible to say whether this deformation is due to the post-metamorphic Ruchi phase, or is the result of the last increments of the Calanda phase. In any case it represents a relatively small amount of strain.

Although the shapes of the individual magnetites are undeformed and euhedral the overall distribution of magnetites is not uniform but appears linked to the concentric elliptical rings traced by the chamosite layers in the ooids. Individual magnetite grains lie within these layers (Fig. 3b) in geometries which produce

elliptical rings of coarse-grained magnetite (Fig. 3c, 3d), or complete elliptical filled-in shells of fine-grained magnetite (Fig. 3e).

To summarize, the mineral assemblages in the rocks analyzed are thought to have developed in the following manner:

1. Growth of hematite and chamosite ooids in a calcareous mud during a diagenetic stage (probably early). A possible source for the iron is alteration on the emerged Bohemian massif.
2. Burial and deformation of the rocks (Calanda phase) with recrystallization of the chamosite and calcite.
3. Metamorphic event with growth of siderite within chamosite ooids and magnetite in both chamosite and hematite ooids.

Magnetic mineralogy

The magnetic properties of the two major types of oolitic limestones were investigated in order to determine which magnetic minerals carry the remanences in each sample and which contribute to the magnetic susceptibility anisotropy. Standard paleomagnetic stability tests were applied to the natural remanences. New remanences were then induced in certain samples in the laboratory and the behavior of these remanences was studied at high and low temperatures.

Measurement of remanence

The natural remanent magnetizations (NRM) which these rocks acquired during their formation or subsequent modification were measured in selected samples using a Digico complete results spinner magnetometer. For the weakest samples a 3-axis ScT cryogenic magnetometer was used. The NRM intensities of the oolitic limestones ranged from 10^{-3} to 10^{-4} A/m.

Alternating-field demagnetization characteristics

The stabilities of the natural remanences were tested by the standard paleomagnetic technique of observing the resistance of the remanence when placed in strong alternating magnetic fields. The alternating field (AF) demagnetization characteristics of representative specimens were determined using a two-axis tumbler for peak fields up to 60 mT (Fig. 5). The Type I specimens contain almost no low coercivity components and in peak fields of 60 mT as much as 75% of the NRM still remains. On the other hand, the Type II limestones show an initial soft component which is removed by peak fields of 10 mT. The reduction in intensity with increasing demagnetizing field is gradual between 10 and 40 mT, after which only about 15% of the NRM still remains.

Thermal demagnetization characteristics

An alternative stability test consists of observing the resistance of the NRM to demagnetization by heating. A number of samples were thermally demagnetized using a progressive, stepwise technique. As a control of whether the magnetic

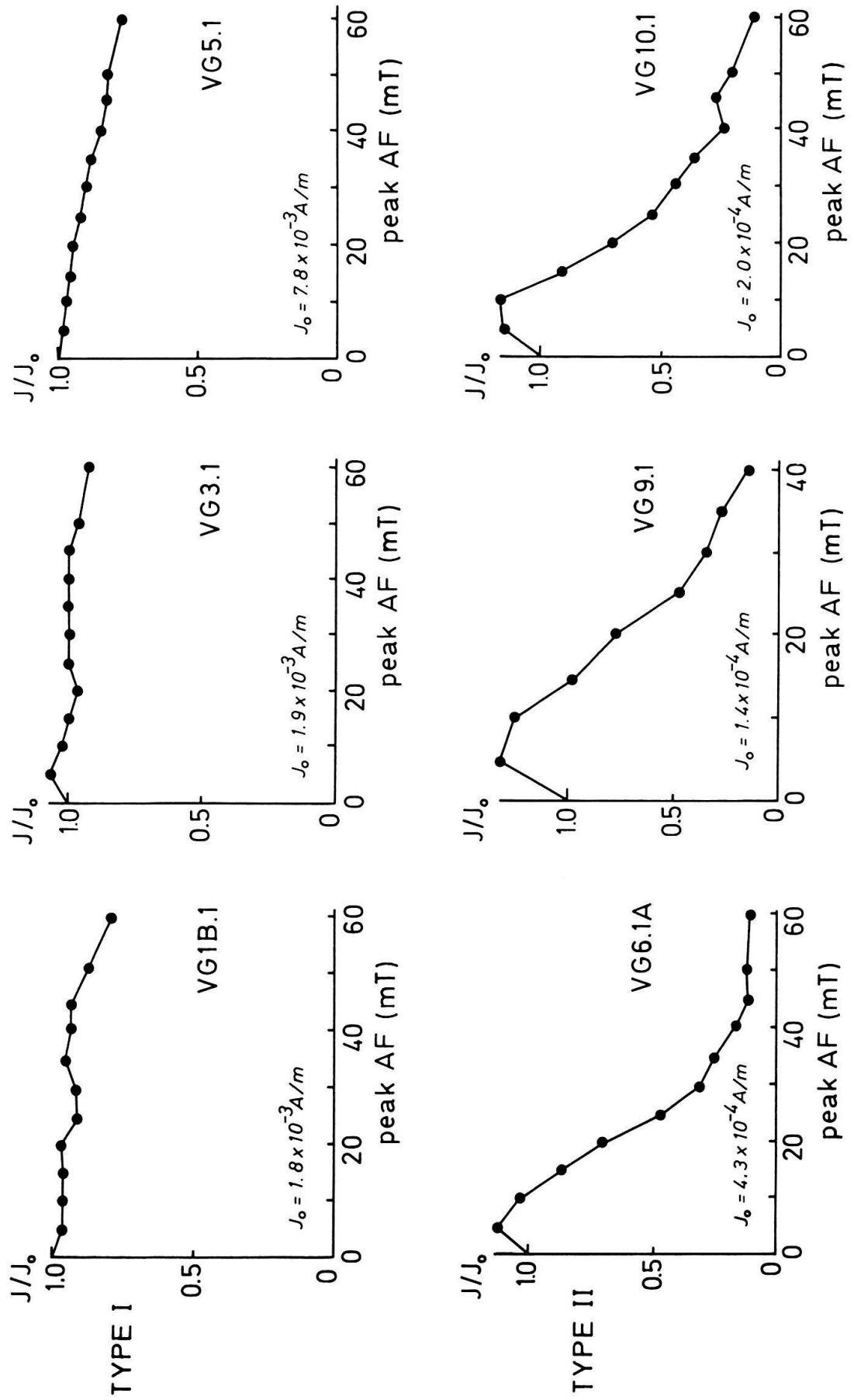

Fig. 5. The reduction of remanent intensity J of oolitic limestone samples during alternating field (AF) demagnetization. The remanence is normalized in terms of the initial value J_o. Type I is a hematite-rich oolite and Type II is a magnetite-rich oolite.

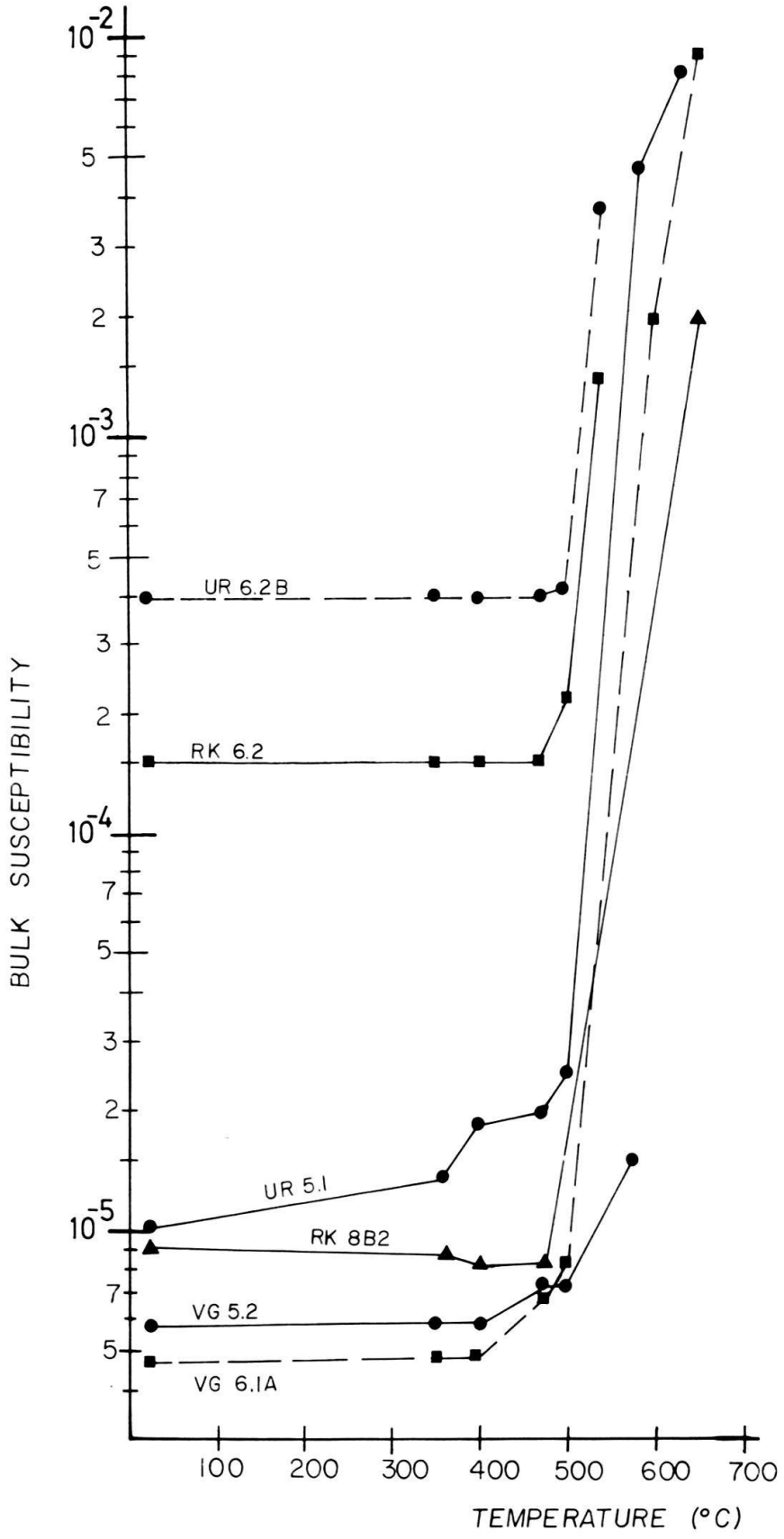

Fig. 6. Change in bulk susceptibility of oolitic limestone samples during laboratory heating to 650 °C. The susceptibility (dimensionless) is given in Standard International (SI) units.

minerals were altered during heating, the bulk susceptibility values were measured on an inductance bridge after each heating stage (Fig. 6). In both Type I and Type II rocks a large change in bulk susceptibility is found upon heating above 425 °C. A corresponding large increase in remanent magnetization intensity was often observed above this temperature on the thermal demagnetization curves. We interpret this as a mineralogical change caused by the breakdown of chamosite, an iron phyllosilicate, with the consequent formation of magnetite at temperatures of 425 °C. Similar effects have been described from the Rose Hill dolomitic sandstone of Maryland (BARRIE et al. 1980). As a result, thermal experiments could not be carried out at higher temperatures without altering the original mineralogy of the limestones.

Thermal demagnetization of NRM and of isothermal remanent magnetization (IRM)

The thermal demagnetization curves for Type I samples show a gradual decrease in magnetization intensities for temperatures up to 400 °C (Fig. 7). A few samples were given an isothermal remanent magnetization (IRM) in fields of 1.2 T (tesla) and then thermally demagnetized stepwise. The IRM intensities of the Type I samples decrease gradually to temperatures of up to 400 °C in the same style as the NRM. The NRM in these samples is probably carried by the same mineral fraction as that carrying the IRM.

Type II specimens show a large change in NRM intensity below 300 °C. The decay during thermal demagnetization of IRM in the same samples is more gradual and 50% of the IRM remains after temperatures of 425 °C; at that temperature only 10% of the NRM still is found. Apparently, during acquisition of the IRM, a different mineral phase was magnetized than that which carries the NRM in these specimens.

A few Type II specimens contain pyrrhotite. Upon thermal demagnetization a significant drop in intensity is observed between 300 °C and 350 °C in both the NRM and IRM curves (Fig. 7, samples UR2.4A, UR2.5). This agrees well with the blocking temperatures reported for natural pyrrhotites (SCHWARZ & HARRIS 1970). Above 350 °C the unblocking characteristics are typical of Type II samples.

We conclude from these thermal experiments that only a single magnetic phase is present in the Type I rocks. On the other hand, two phases (and sometimes three) are present in the Type II specimens: a low blocking temperature phase carrying the NRM, an additional higher blocking temperature phase which acquires IRM, and sometimes a moderate blocking temperature phase due to pyrrhotite.

Acquisition of isothermal remanent magnetization (IRM)

Selected unheated samples from each rock type were given an IRM in progressively increasing magnetizing fields up to 1.2 T. The behavior of the two groups of specimens differs remarkably (Fig. 8). The Type I specimens reach less than 10% of saturation IRM in magnetizing fields below 0.2 T. The shape of the IRM acquisition curves is concave upwards until about 0.2 T; the IRM then increases rapidly between 0.2 and 0.8 T, and levels off at higher fields but does not reach saturation at

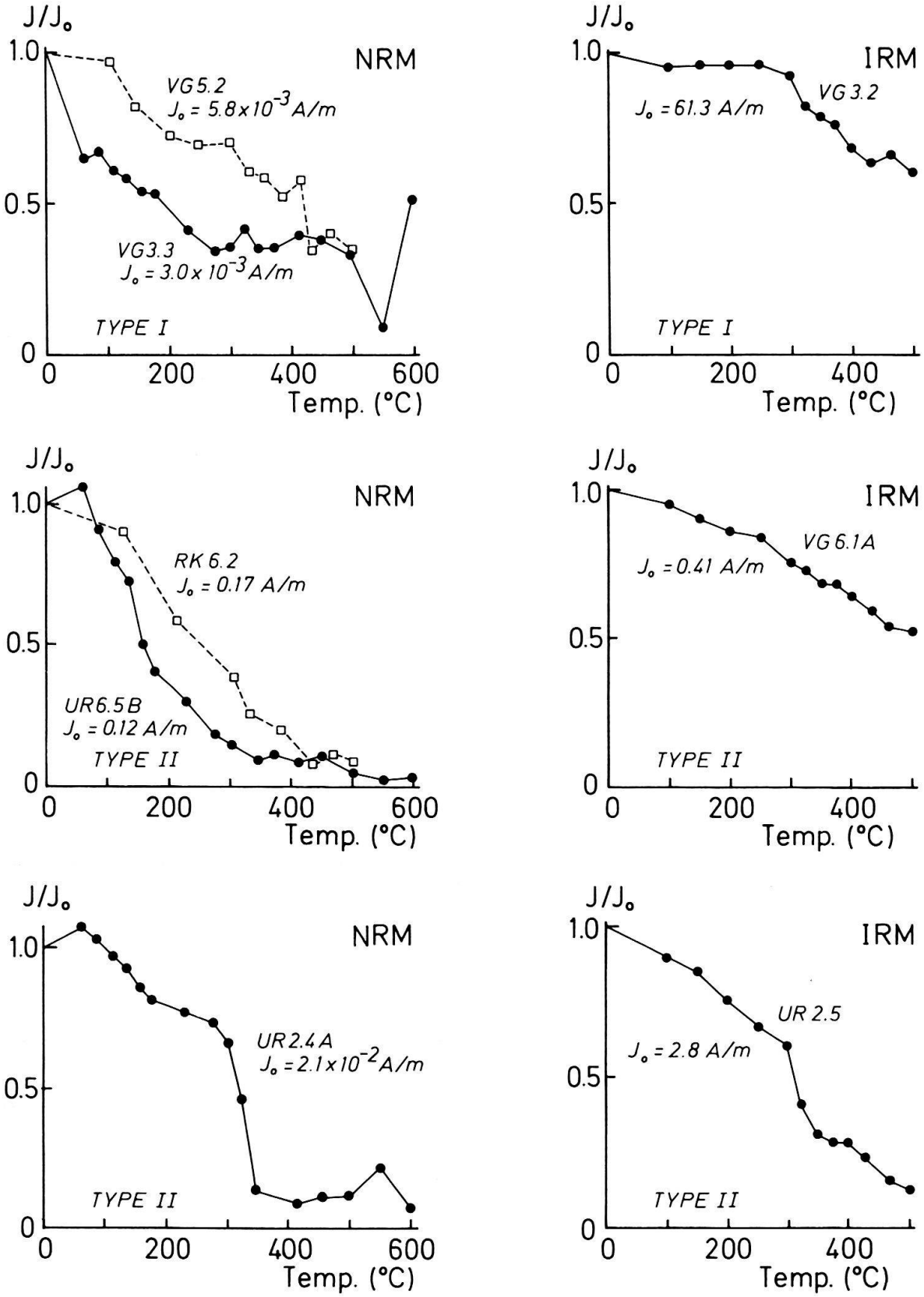

Fig. 7. Thermal demagnetization curves of oolitic limestones. Thermal demagnetization of natural remanent magnetization (NRM) and of isothermal remanent magnetization (IRM) are shown for different oolite types. J and J_0 are as in Figure 5.

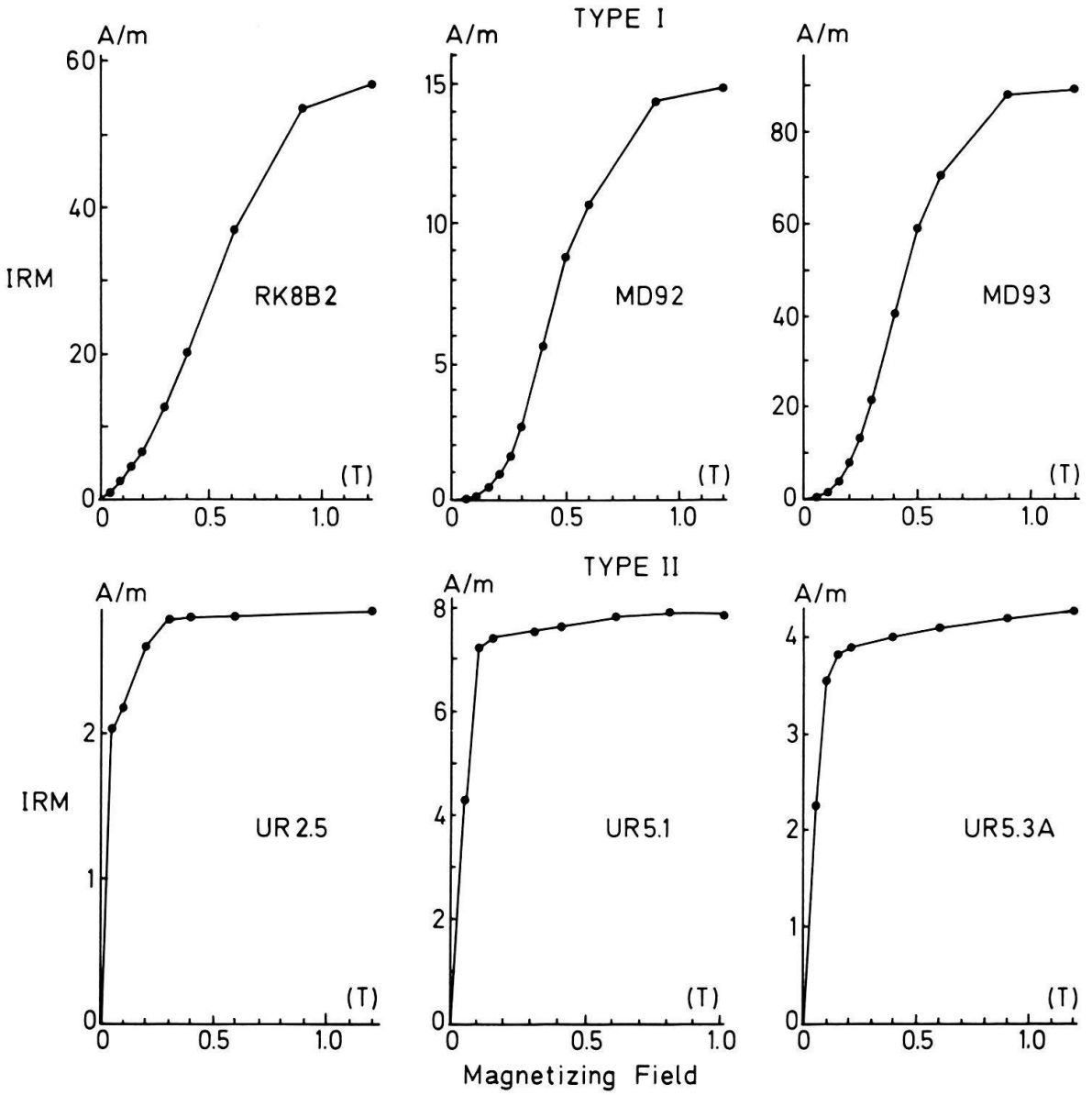

Fig. 8. The acquisition of isothermal remanent magnetization (IRM, in ampères/m) by oolitic limestones in progressively increasing magnetizing fields (tesla).

1.2 T. The thermomagnetic and coercivity observations indicate that the magnetic properties of Type I specimens are probably due to hematite.

The Type II specimens achieved 85–90% of saturation IRM in magnetizing fields of less than 0.2 T. Saturation was generally achieved in fields of 0.35 to 0.5 T. The magnetic mineralogy of Type II specimens is characterized by low and moderate coercivities, but in some Type II specimens higher coercivity components are also found (for example, specimen UR5.3A, Fig. 8).

Low temperature experiments

It is possible to identify the magnetic minerals in a rock by observing the occurrence of low temperature magnetic transitions related to magnetocrystalline

effects during thermal cycling between room temperature and liquid nitrogen temperature (−196 °C) (NAGATA et al. 1964). A few samples were given an IRM in 1.2 T at room temperature. The magnetization of all three components of remanence was monitored continuously using a device designed by HEINIGER & HELLER (1976). The behavior of the magnetization of Type II samples during cooling to liquid nitrogen temperature and rewarming to room temperature is typified by specimen UR5.4B (Fig. 9a). During cooling, the IRM is substantially reduced at temperatures below −140 °C corresponding to the magnetocrystalline anisotropy transition for magnetite. During rewarming to room temperature about 75% of the original IRM is recovered across the magnetite transition. The same sample was then given a 1.2 T IRM at liquid nitrogen temperature and this magnetization was monitored during warming to room temperature (Fig. 9b). About 70% of the low temperature IRM is lost at a temperature between −140 and −150 °C.

An IRM in a 1.2 T field was given to a Type I specimen at liquid nitrogen temperature (Fig. 9c). In this case the IRM decays steadily during rewarming to room temperature and no large rapid decrease in magnetization is observed. This indicates that multidomain magnetite is not present. The progressive decay during warming of the low temperature IRM may be due to the thermal unblocking of hematite or single domain magnetite. The coercivity data (Fig. 8) imply that the effect is due to hematite.

According to NAGATA et al. (1964) pure hematite exhibits a magnetic effect (the Morin transition) at temperatures of −20 °C to −50 °C. This effect is suppressed by even minor amounts of impurity. This would account for the absence of any slope change or other effect in the observed thermomagnetic curves on our natural samples.

Summary of rock magnetism

The magnetic mineralogy appears to be simple in the Type I rocks. The AF demagnetization characteristics and the similarity in the thermal demagnetization curves of both the IRM and the NRM suggest that hematite is the only magnetic phase present in the Type I specimens. Their IRM acquisition curves demonstrate

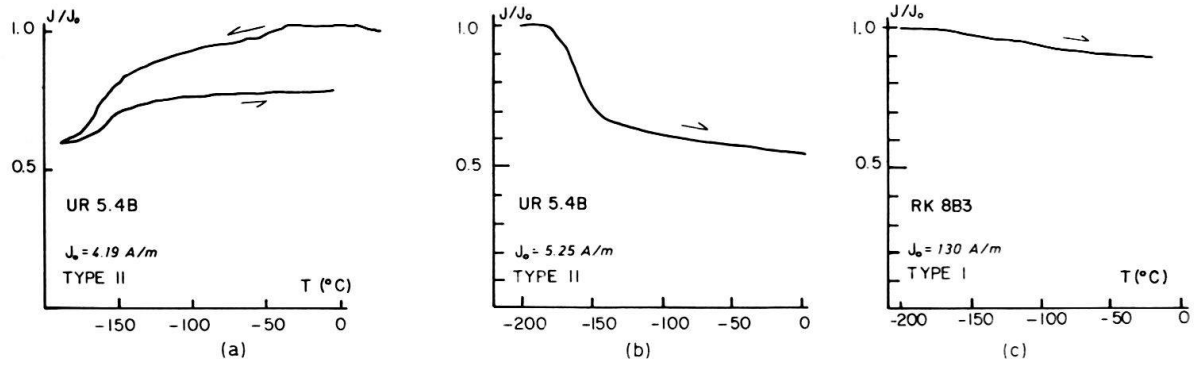

Fig. 9. a: Low-temperature thermal cycling of IRM acquired by a Type II oolite at room temperature.
b: Change of IRM acquired at liquid nitrogen temperature by a Type II oolite during rewarming to room temperature.
c: As in b; Type I oolite.

that little or no magnetite is present in these rocks. Following DUNLOP (1972) it appears that the shapes of these curves are due entirely to a combination of hematite particles ranging from coarse grain sizes down to fine grains that carry remanence at low temperature but are superparamagnetic at room temperature.

The magnetic mineralogy of the Type II rocks is more complex. The IRM acquisition curves and low temperature studies demonstrate the presence of multidomain magnetite. However, the thermal demagnetization curves of both the NRM and the IRM suggest the additional presence of pyrrhotite in some samples. Furthermore there is a discrepancy between the thermal demagnetization of NRM and of IRM in the samples without pyrrhotite. It appears that, although magnetite carries the NRM in these rocks, another magnetic phase which is also present in the rock becomes magnetized during acquisition of IRM. This is also suggested by the fact that the IRM acquisition curves do not saturate in fields of 1.2 T. Ferromagnetic goethite is common in some limestones and can have coercivities in excess of 5 T, but its Curie temperature is less than 150 °C. The thermal demagnetization curves indicate it is not present in these oolitic limestones. Probably the ferromagnetic minerals in Type II rocks are predominantly magnetite with additional small quantities of hematite.

Magnetic susceptibility anisotropy

The magnetization component (J_i) produced by orthogonal magnetic field components (H_j) in an anisotropic rock is given by

$$J_i = k_{ij} H_j .$$

The second order tensor k_{ij} describes the anisotropic susceptibility of the rock and is represented geometrically by a triaxial ellipsoid whose principal axes are the maximum (k_{max}), intermediate (k_{int}) and minimum (k_{min}) susceptibilities, respectively.

Euhedral magnetites have a cubic crystal structure in which the susceptibility is crystallographically controlled. However, since magnetite grain shapes do not usually bear any relation to its crystallographic easy axes, a distribution of euhedral magnetite grains generally shows no preferred orientation of crystallographic axes and hence no anisotropy due to crystallographic effects.

Magnetite has a strong spontaneous magnetization and magnetostatic effects at grain surfaces are important. Therefore, the susceptibility anisotropy of magnetite grains is generally shape-dependent and the k_{max}, k_{int} and k_{min} susceptibility axes are parallel to the long, intermediate and short axes of the magnetite grain, respectively. As a result, the susceptibility anisotropy of a magnetite-bearing rock is due to the preferred orientation of an assemblage of magnetite grains.

The spontaneous magnetization of hematite is so low that magnetostatic effects are unimportant. Magnetocrystalline anisotropy is predominant with k_{max} and k_{int} axes lying within the hematite basal plane and k_{min} axes perpendicular to it. Since hematite often shows parting along its basal plane, a preferred orientation of hematite basal planes leads to a strong magnetic susceptibility anisotropy with k_{min} axes normal to the basal planes (BHATHAL 1971; UYEDA et al. 1963).

Anisotropy measurement

A total of about 160 samples were used in this study. They were cut to length-to-diameter ratios of 0.88 since excessive deviations can lead to anomalous fabric determination using spinner magnetometers (KENT & LOWRIE 1975).

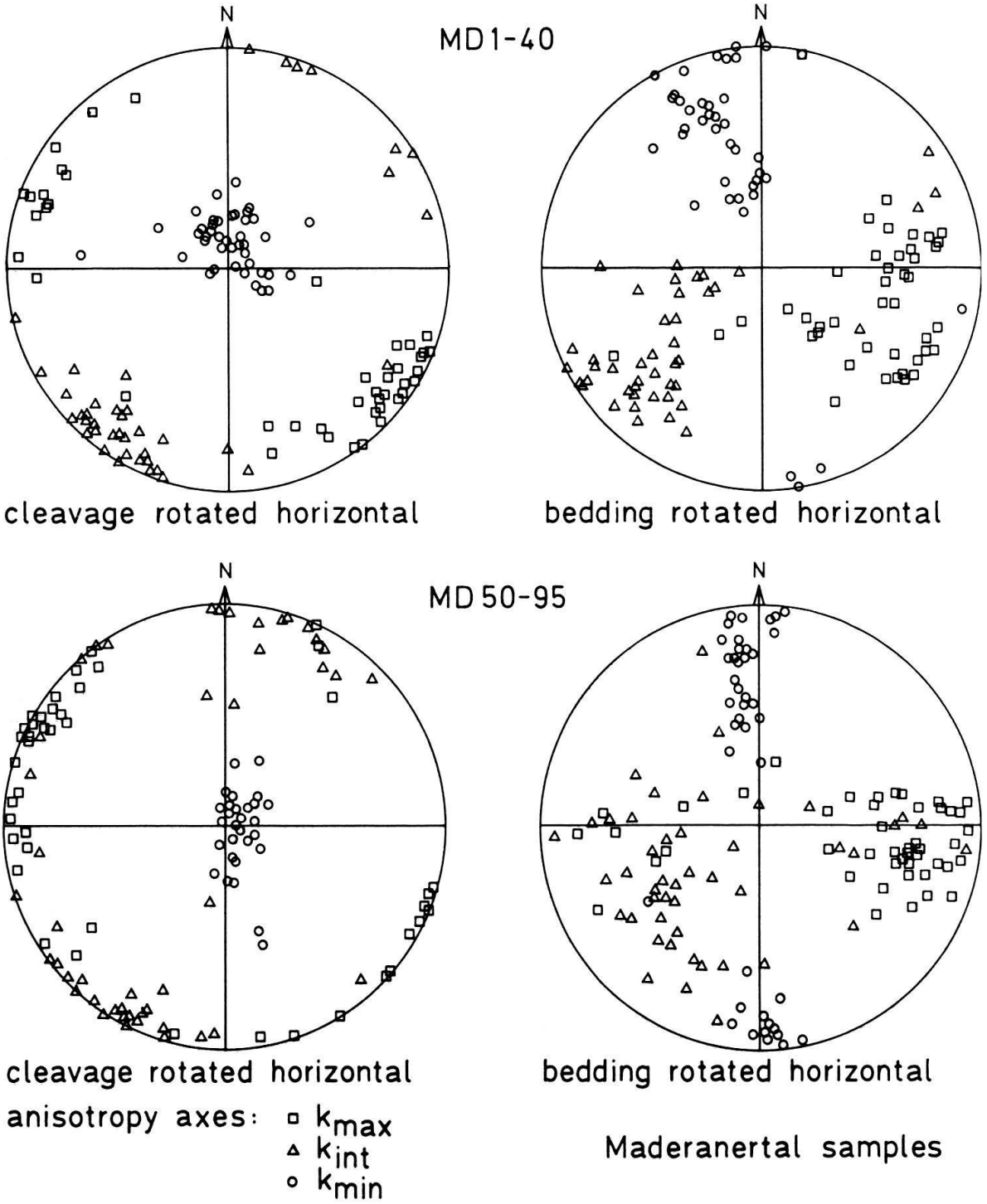

Fig. 10. Relationship of magnetic susceptibility principal axes ($k_{max} > k_{int} > k_{min}$) with respect to cleavage and bedding in two folds at Maderanertal, site 3. The k_{min} axes group perpendicular to cleavage but show no relationship to bedding.

The low-field susceptibility anisotropy of all samples was measured on both the Digico spinner magnetometer and the cryogenic magnetometer. The results from the Digico spinner were combined with bulk susceptibility values obtained on an

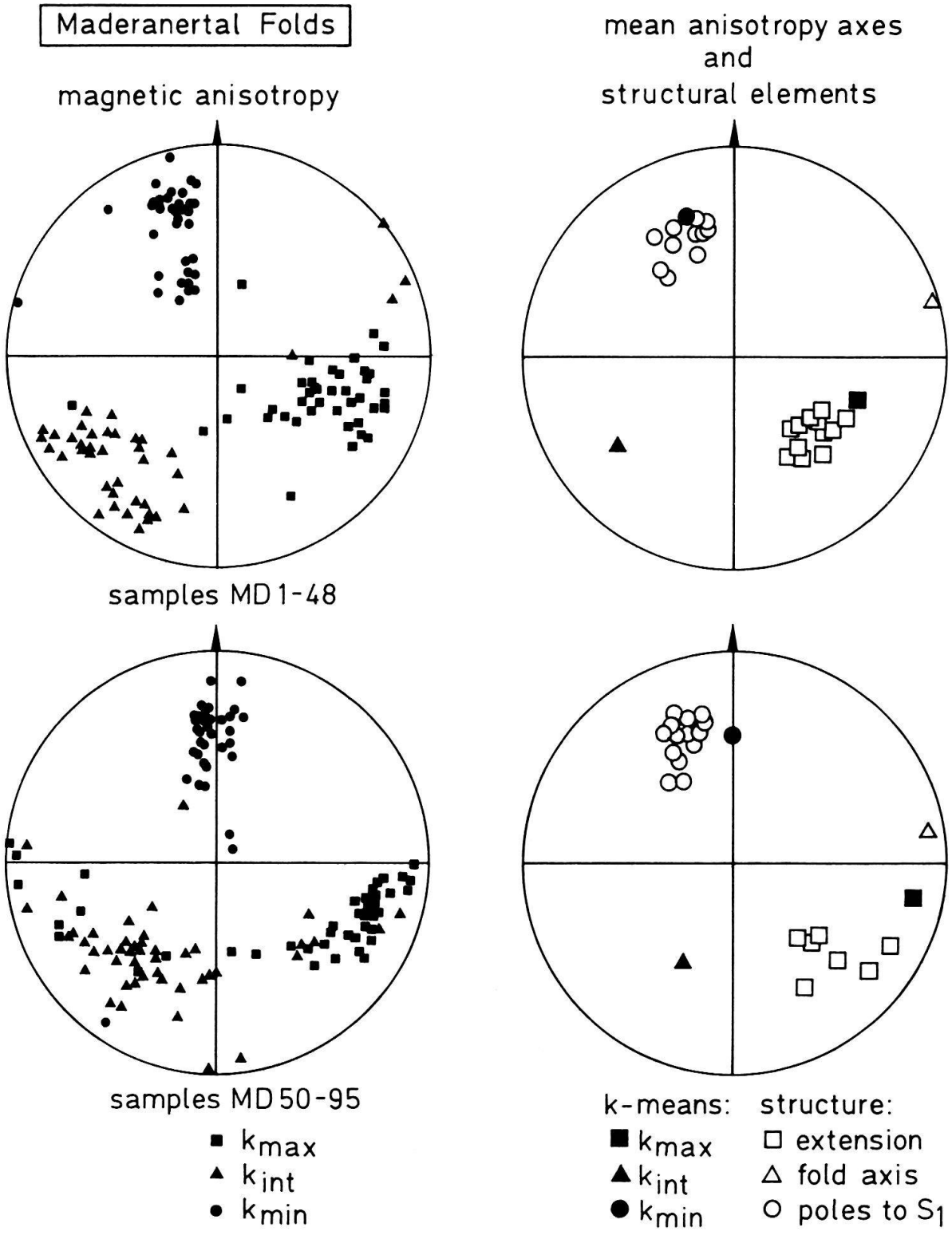

Fig. 11. Comparison of the principal magnetic anisotropy and structural elements for the Maderanertal folds. S_1 = Calanda phase cleavage.

AC inductance bridge in order to find the principal susceptibility values and directions. The measurement of susceptibility anisotropy on the cryogenic magnetometer was carried out using the procedures outlined by SCRIBA & HELLER (1978). Comparisons between instruments were evaluated by measurements of different paramagnetic salts.

Directional data at sites

Magnetic susceptibility data for undeformed sedimentary rocks commonly show that k_{min} axes are normal to bedding and that k_{int} and k_{max} axes may or may not cluster in a particular direction (HROUDA & JANAK 1971, HAMILTON 1963, HAMILTON & REES 1970, REES 1965). Where the fabric results from deformation (HROUDA 1978, HROUDA & JANAK 1976, KLIGFIELD et al. 1977, HENRY 1973, KLIGFIELD et al. 1981, GRAHAM 1966, HELLER 1973, RATHORE 1979) the k_{min} axes are normal to cleavage and k_{max} axes are usually parallel to mineral extension lineations, where developed.

The magnetic susceptibility axes of all specimens from two folds at Maderanertal (MD1-40 and MD50-95) have been rotated so that the cleavage and the bedding are

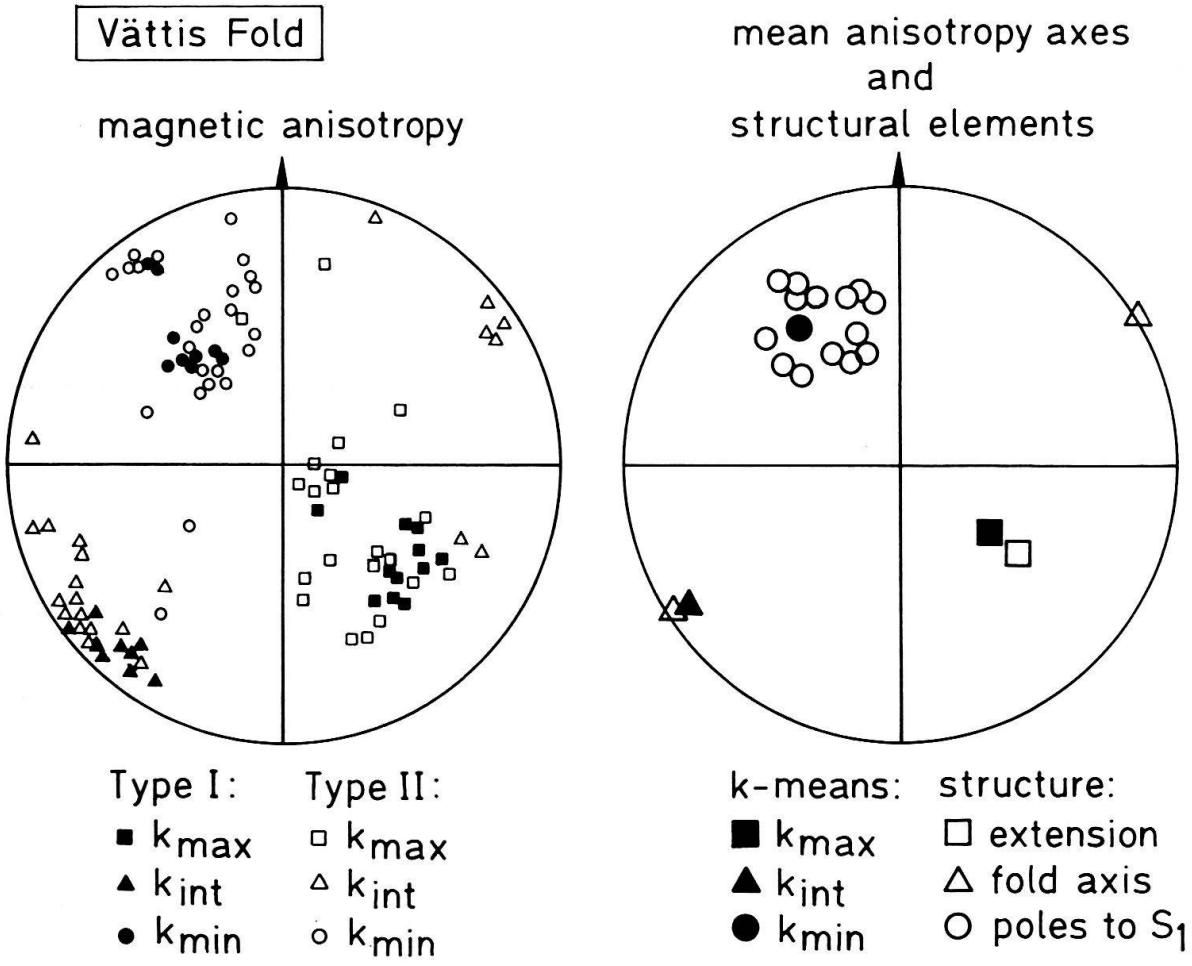

Fig. 12. Comparison of the principal magnetic anisotropy and structural elements for the Vättis fold. Principal directions from the Type I and Type II layers do not differ. S_1 = Calanda phase cleavage.

brought respectively into the horizontal plane of the stereographic projection (Fig. 10). It is seen that the k_{min} axes cluster near the pole to the cleavage of each sample rather than near the pole to bedding. We conclude that the orientations of the magnetic susceptibility principal axes are related to the deformation in these rocks, and not to sedimentary processes.

Comparison of the fold structures with the susceptibility axes clearly demonstrates the tectonic control of the susceptibility patterns (Fig. 11).

At Vättis (Fig. 12), Urbachtal (Fig. 13) and in the two folds at Maderanertal (Fig. 11) the following features are observed: a) the k_{min} axis of each specimen is nearly perpendicular to the cleavage and to the XY plane of the finite strain ellipsoid (X > Y > Z) determined from the shapes of the deformed oolites (see discussion below); b) the k_{max} axis of each specimen is nearly parallel to the X strain direction and to the mineral elongation lineation within the cleavage; and c) the k_{int} axis of each specimen is either close to the fold axis or to the Y direction of the finite strain ellipsoid, if these do not coincide. Together, the data form clusters of k_{max}, k_{int} and k_{min} axes parallel to the X, Y and Z strain axes, respectively. There appear to be no major differences in the directions of the principal susceptibilities between the hematite (Type I) layers and the magnetite (Type II) layers (Fig. 12).

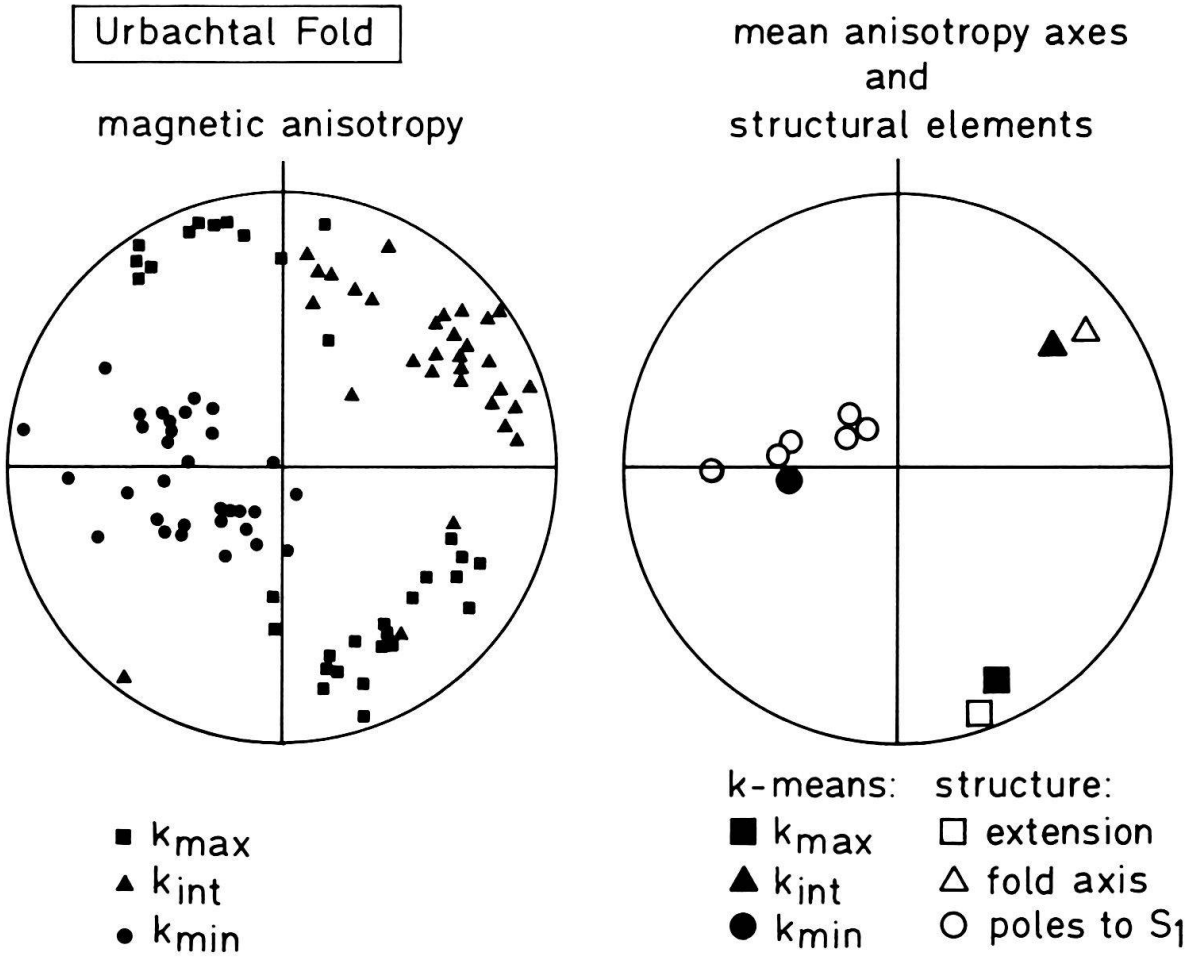

Fig. 13. Comparison of the principal magnetic anisotropy and structural elements for the Urbachtal fold. S_1 = cleavage.

The data from Färnigen (Fig. 14) are more difficult to interpret. The overturned limb of the syncline shows elongation of the oolites in a direction which is down-dip of the axial planar schistosity. The normal limb from which our samples come consists of a series of small scale folds with large strain variations within them (TAN 1969). The magnetic susceptibility directional data are more scattered than at the other sites. A crude grouping of k_{max} axes is subparallel to the down-dip extension lineation of the oolites as measured in the inverted limb. Two separate clusters consisting of both k_{min} and k_{int} axes can be distinguished. They are parallel to the fold axis direction and to the poles to schistosity. The classification scheme of KLIGFIELD et al. (1977) can be used to compare the directional groupings of the susceptibility axes with the shapes of the individual susceptibility ellipsoids. The ellipsoids are largely prolate, having nearly equal k_{min} and k_{int} axes (Type II–IIIa anisotropy).

These results can be interpreted in the following way. It appears that the magnetic susceptibility results are more characteristic of the higher constrictional strains associated with the inverted limb region than with those of the normal limb (flattening to plane strains). TAN (1969) reports the additional presence here of a kaolinite oolite. The differences between our magnetic results and those reported by TAN for the strain may be due to the different responses to deformation of the two oolite types in this area. Further work is needed to clarify this problem.

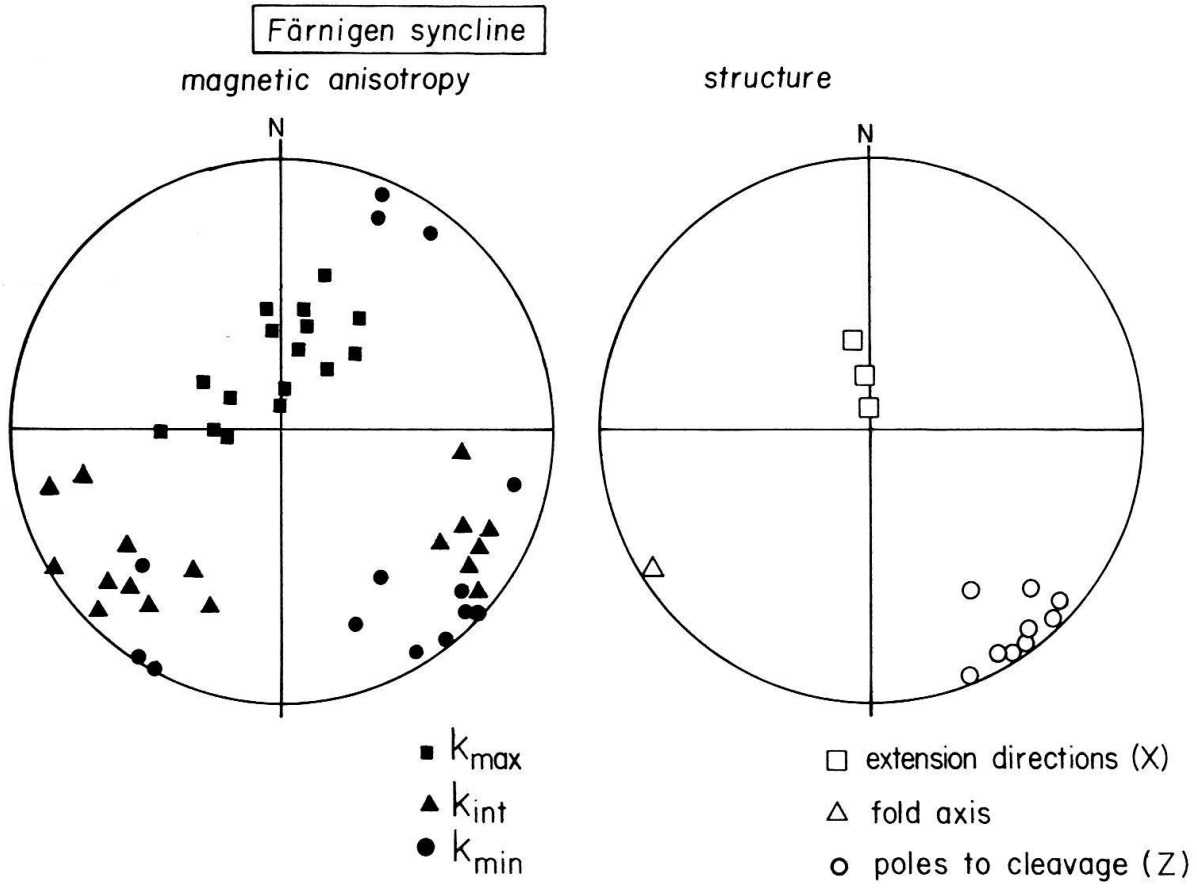

Fig. 14. Comparison of the principal magnetic anisotropy and structural elements for the Färnigen syncline. S_1 = cleavage.

Minerals causing magnetic anisotropy

The magnetic fabric results can only be related quantitatively to a deformation mechanism if the source of the magnetic anisotropy is known (OWENS 1974). The minerals present in our specimens have diamagnetic (calcite), paramagnetic (chlorite, chamosite and clays) and ferromagnetic (magnetite and hematite) susceptibilities (OWENS & BAMFORD 1976, OWENS & RUTTER 1978, PARRY 1971). In order to consider the effects of deformation on the orientations of the magnetites and hematites, it is necessary to rule out the presence of large contributions to the susceptibility anisotropy due to the diamagnetic and paramagnetic minerals also present in the rocks. If diamagnetic and paramagnetic minerals coexist in a rock, the contribution to the susceptibility of the paramagnetic minerals generally is much stronger than that of the diamagnetic minerals. The problem in these oolitic limestones becomes one of examining the effects due to anisotropic paramagnetic and ferrimagnetic mineral fractions.

Strong-field torque measurements

Measurements over a range of higher fields allow the presence of different components to be recognized and sometimes resolved (PARRY 1971, OWENS & BAMFORD 1976). The torque experienced by an anisotropic sample in a strong magnetic field results from either shape alignment of grains with a preferred orientation of long axes (as in the case of magnetite) or from preferred alignment of crystal axes (as in hematite) (BHATHAL 1971).

In the case of magnetite, in a field strong enough to produce saturation magnetization the anisotropy is due to statistically preferential alignment of grain long axes. The difference in energy of saturation magnetization (J_s) can be written:

$$E = \frac{1}{2} v J_s^2 (N_a \cos^2\Theta + N_b \sin^2\Theta)$$

(STACEY 1963, BHATHAL 1971) where θ is the angle of the applied field H to the specimen reference direction, v is the volume of the specimen, and N_a and N_b are the demagnetizing factors of the ellipsoid (STONER 1945, OSBORN 1945). The torque in the plane of measurement T can be obtained by differentiating the energy expression:

$$T = \frac{-\mathrm{d}E}{\mathrm{d}\Theta} = -\frac{1}{2} v J_s^2 (N_b - N_a) \sin 2\Theta .$$

It is seen that the amplitude of the torque curve does not depend upon the value of the applied field once magnetite has reached saturation magnetization.

For hematite, STACEY (1963) proposed that the torque in saturation fields depends on the angle which the basal plane containing the saturation magnetization makes with the applied field. He obtained:

$$T = -J_s H \sin 2\Theta .$$

PORATH & CHAMALAUN (1966) proposed a different expression given by:

$$T = J_s H (\sin\Theta \sin^2\phi)/(1 + \tan^2\Theta \cos^2\phi).$$

In this case θ is the angle the applied field makes with the reference direction and Φ is the angle the basal plane makes to the plane of rotation of the torque measure-

ment. For hematite that has reached saturation magnetization the torque amplitude increases proportionally with applied field H.

For diamagnetic and paramagnetic minerals the torque T experienced by the sample is given by:

$$T = \frac{1}{2} vH^2[(X_{11} - X_{22})\sin 2\Theta - 2X_{12}\cos 2\Theta],$$

where v is the volume of the specimen and X_{ij} are the susceptibility components in the plane of measurement (OWENS & BAMFORD 1976). Thus the torque amplitude in the plane of measurement varies with the square of applied field (H^2), if only paramagnetic and/or diamagnetic minerals are involved.

From the above expressions it is seen that if the field H is increased while the saturated sample remains in a fixed position, the torque for magnetite will not change, that for hematite will vary with H, and that for paramagnetic minerals will vary with H^2.

The torque in applied fields at strength up to 1.2 T was measured on selected samples of Type I layers using a high field torque meter of the type described by BANARJEE & STACEY (1967). The torque versus H and torque versus H^2 curves obtained are shown in Figure 15a.

The T versus H^2 curves are not linear and we conclude that paramagnetic minerals alone cannot explain the anisotropies observed in the Type I layers.

Rotational hysteresis

Rotational hysteresis W_r is the work done when a sample is rotated through 360°. It is due to discontinuous changes in magnetization at intermediate field strengths (MANSON et al. 1979, DAY et al. 1970). W_r for magnetite characteristically rises sharply to a maximum at a field strength of about 0.2 T and then decreases with increasing field strength. Different W_r versus H curves are possible for hematite due to variability of the coercivity. Broad peaks at 0.7 T decaying slowly at higher fields are generally observed for specularite-bearing sandstones. For finer grained specu-

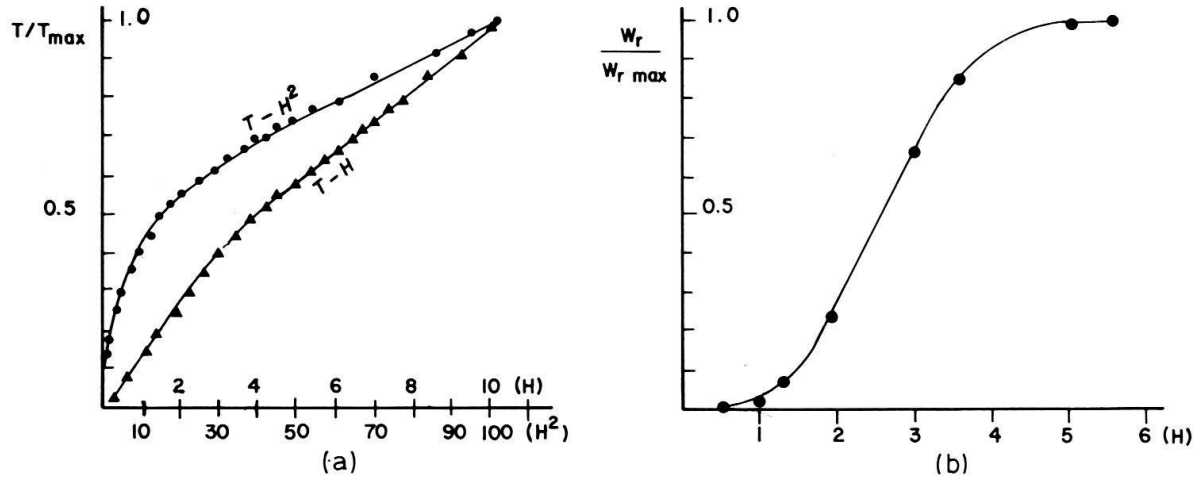

Fig. 15. a: Variation of magnetic torque T, normalized in terms of the maximum torque T_{max}, with increasing magnetic field H and with the square of the field H^2. For emphasis, the field units are kilogauss in this diagram.

b: Field dependence of rotational hysteresis W_r, normalized in terms of its maximum value W_{rmax}.

larite and pigmentary hematite the rotational hysteresis often continues to increase even above fields of 1.5 T (PARRY 1971, BROOKS & O'REILLY 1970).

In Type I samples W_r increases in fields up to 0.4 T and then persists (Fig. 15b). No maximum that could be ascribed to magnetite is observed. The shape of the observed curve again suggests that the mineral causing the high-field torque characteristics is hematite. This result is in good agreement with the evidence presented from the IRM curves which show the absence of magnetite in these samples.

On the other hand hematite is expected to yield a torque curve which varies only with H. Although linear parts to the T versus H curves are seen (Fig. 15a) the curve is more complex. This departure from linearity in the T versus H curves of the Type I specimens is probably due to the effect of incomplete saturation of hematite in the magnetic fields available (up to 1.2 T).

In summary, the Type I specimens are particularly attractive for a study of the relationship between magnetic susceptibility anisotropy and deformation because the susceptibility anisotropy appears to be produced by hematite alone.

Mimetic fabric and susceptibility anisotropy

It is clear from Figures 10–14 that the magnetic susceptibility anisotropy and the structural elements at each site are closely related. The way in which the magnetic particles respond to the deformation can be understood quantitatively from the "strain response model" of OWENS (1974). We begin by examining the relationships of the magnetite and hematite grains to the deformed shapes of the ooids.

Distribution of magnetites in Type II samples

The mimetic fabric of magnetite has important consequences for the susceptibility anisotropy. A uniform non-interacting assemblage of equidimensional magnetite grains has isotropic susceptibility because of the lack of shape effects for the individual grains and a lack of preferred crystallographic orientation. However, the grains of magnetite in the Type II specimens are so densely packed that they cannot be regarded as non-interacting. Many grains lie within one diameter of their nearest neighbors (Fig. 3b) and in the case of the fine-grained magnetite found in opaque shells (Fig. 3e), the grains must be almost touching. As a result, we have an effective shape effect due to the interaction of grains which produces an equivalent magnetic anisotropy to that of an ellipse of magnetite. It is therefore possible to use these distributions of mimetically recrystallized magnetites to directly determine the shape of the deformed ooids and hence the finite strain in the rock. This is possible because shape demagnetization factors (and therefore the magnetic susceptibility anisotropy) in magnetite grains are directly related mathematically to the ellipsoidal shape of the grain (OSBORN 1945, STONER 1945).

Distribution of hematites in Type I samples

The distribution of hematite basal planes is the important factor in controlling the susceptibility anisotropy of the hematites. In thin and polished section photomi-

crographs (Fig. 3), the hematite basal planes are seen to roughly follow the layers of the deformed ooids.

Whatever the origin of the hematites, we believe that the present distribution of hematites is largely controlled by the shapes of the ooids. Hematites act as tangent planes to the curving ooid surfaces and layers and their preferred orientation must reflect the overall shape of the ooid. Thus a very strong preferred orientation of hematite basal planes occurs when the ooids are strongly deformed whereas a spherical ooid would have in effect no preferred hematite orientation. As a result the preferred orientation of hematite basal planes is controlled by the deformation. The magnetic susceptibility anisotropy (which is determined by hematite basal plane orientation) is again directly related to the ooid shapes.

Correlation with strain

GRAHAM (1954) was the first to suggest that magnetic susceptibility anisotropy could be used as a petrofabric indicator in rocks. Since his early work much progress has been made in examining the qualitative (HROUDA & JANAK 1976, GRAHAM 1966, VAN DEN ENDE 1977, HENRY 1973, HELLER 1973), semiquantitative (KLIGFIELD et al. 1977, HROUDA 1979, HROUDA 1976) and quantitative (OWENS 1974, WOOD et al. 1976, KNEEN 1976) relationships between strain and magnetic anisotropy in rocks. Work in hematite-bearing slates has demonstrated that under favorable conditions it is possible to determine finite strain measurements directly from magnetic susceptibility measurements (WOOD et al. 1976, RATHORE 1979, KLIGFIELD et al. 1981).

We have shown that there are no directional differences between the Type I and Type II specimens (Fig. 12); both show a clear directional correspondence between strain and magnetic principal axes (Fig. 11–13). However it was noted at Färnigen that differences in the magnetic mineralogy can seriously affect this simple relationship between strain and magnetic anisotropy. The Type I specimens (hematite-bearing oolites) were selected to compare quantitatively their strain and magnetic fabrics because of their simple magnetic mineralogies, their abundance in the field, and because the ooids were easy to measure from enlarged thin section photographs. In addition, the hematite oolites also show less pressure solution effects and hence provide higher accuracy in the strain determinations (PFIFFNER 1980).

Strain analyses

The techniques of strain analysis in oolitic rocks consists of measuring the shape (axial ratio) and orientation of the ooids and/or of measuring the distance between the centers of neighboring ooids (PFIFFNER 1980). As the initial fabric of the ooids strongly affects the final (deformed) fabric, a knowledge of the initial state increases the accuracy of the analysis. The initial fabric of the undeformed oolites can be summarized as follows (PFIFFNER 1977, 1980): The ooids are ellipsoidal (mean axial ratio 1.4, ranging from 1 to 2.3) and the long axes of the ooids do not show any preferred orientation (i.e. uniform distribution).

The methods used in this study include:

a) Measuring long and short axes of the individual ooids; the arithmetic means of these ratios can then be converted to strain ellipse axial ratios by means of the curves given in PFIFFNER (1980) (reduced means method).
b) Measuring the dimensions of the individual ooids parallel and perpendicular to the trace of the plane of flattening. By using the arithmetic mean of the logarithms of the individual ratios one can estimate the strain ellipse axial ratio (ROBIN 1977).

The advantage of method (a) is that it was developed for this particular rock type while method (b) is very rapid. Variations in the state of strain existing within sampling sites (PFIFFNER 1980) have been also noted in previously reported magnetic anisotropy results (KLIGFIELD et al. 1977, KLIGFIELD et al. 1981). For correlation purposes it was therefore necessary to undertake the strain measurements on the exact sample as that used for the susceptibility measurements. Thin sections were cut from three mutually perpendicular planes in each of nine magnetic cores analyzed. Hence large scale heterogeneities due to strain variation were avoided and the strain values are thought to be representative of the state of strain in the cylindrical samples used for magnetic measurements. The samples were chosen in order to obtain a large variation in both the type as well as intensity of strain. Any three planar perpendicular sections are sufficient to completely determine the three-dimensional shape of the finite strain ellipsoid (RAMSAY 1967, SIDDANS 1980). From each of the nine samples the strain ratio R_s and the angle between the long axis of the strain ellipse and a reference direction Φ were measured in each of the three perpendicular planes. The orientations and values of the principal strains were obtained with the aid of the computer program of SIDDANS (1971). The input from each of the three planar sections overdetermines the solution and gives an "error" estimate (the internal inconsistency). The principal strains along with the internal inconsistency in the analyses are given in Table 1.

Table 1: *Finite strain results from cores used for magnetic studies. X', Y' and Z' are in the coordinate system of the thin section measurements. X, Y and Z are in the coordinate system of the principal strains. Error refers to the internal consistency error of the calculation of three-dimensional strains from two-dimensional strain ratios. Φ refer to the angles made by the long dimension of the strain ellipse with the reference axis on each thin section.*

Sample	2-D strain ratios			2-D angles			3-D strain ratios			Error
	X':Y'	Y':Z'	Z':X'	ϕ_1	ϕ_2	ϕ_3	X:Y	Y:Z	Z:X	(%)
MD 5	2.69	3.07	2.49	141	91	1	1.35	1.10	0.67	0.91
9	3.25	4.30	1.35	12	59	88	1.46	1.10	0.62	8.72
18	2.45	3.18	3.45	151	26	80	1.43	1.09	0.64	2.14
19	1.60	2.34	3.65	179	15	91	1.33	1.08	0.70	4.94
26	2.59	2.91	2.08	137	66	25	1.31	1.13	0.68	7.89
62	5.34	5.29	5.59	146	73	29	1.72	1.13	0.51	0.89
64	3.26	3.47	2.75	137	73	17	1.38	1.16	0.63	4.97
69	2.65	3.20	1.70	163	71	35	1.31	1.12	0.68	4.39
88	3.65	5.55	6.55	128	59	22	1.76	1.08	0.53	11.08

Quantitative relationships between strain and anisotropy

The directions of the principal finite strains and of the principal magnetic susceptibilities determined in the same cores are in good agreement with each other. The principal normalized susceptibilities have been plotted against the principal (equal volume normalized) finite strains (Fig. 16 and Table 2). Although the data are somewhat scattered, a linear relationship between strain and magnetic anisotropy is observed over the range of strains indicated.

The principal logarithmic strains $\varepsilon_i = \ln(1+e_i)$ can be determined directly from the normalized principal susceptibility differences (defined such that $M_i = (k_i - \bar{k})/\bar{k}$ where $\bar{k} = (k_{max} + k_{int} + k_{min})/3$) using the relationship $\varepsilon_i = aM_i$ where $a = 5.69$ for the hematite oolites found in the Maderanertal region. It is important to note that

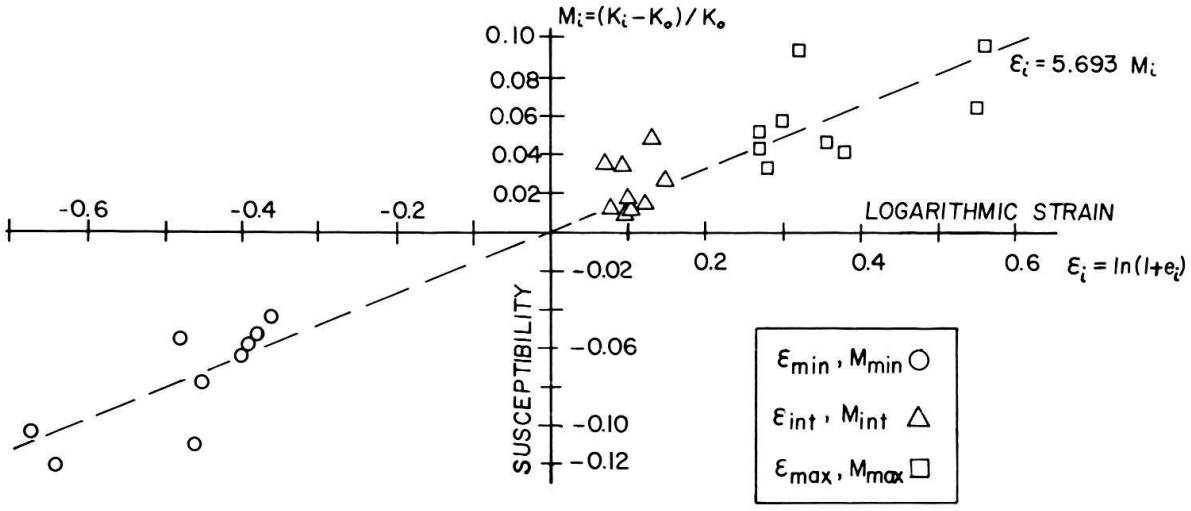

Fig. 16. Correlation of normalized principal magnetic susceptibilities M_i and logarithmic strain ε_i in hematite oolites from Maderanertal.

Table 2: *Finite strain and magnetic susceptibility principal values used in the correlation diagram in Figure 16.*

Sample	ε_1	M_1	ε_2	M_2	ε_3	M_3
MD 5	0.30	0.057	0.10	0.009	-0.40	-0.063
9	0.38	0.041	0.10	0.018	-0.48	-0.056
18	0.36	0.047	0.09	0.036	-0.45	-0.078
19	0.28	0.033	0.08	0.011	-0.36	-0.043
26	0.27	0.048	0.12	0.013	-0.39	-0.058
62	0.55	0.064	0.13	0.049	-0.67	-0.104
64	0.32	0.095	0.15	0.026	-0.46	-0.110
69	0.27	0.042	0.11	0.013	-0.38	-0.052
88	0.56	0.097	0.07	0.037	-0.64	-0.121

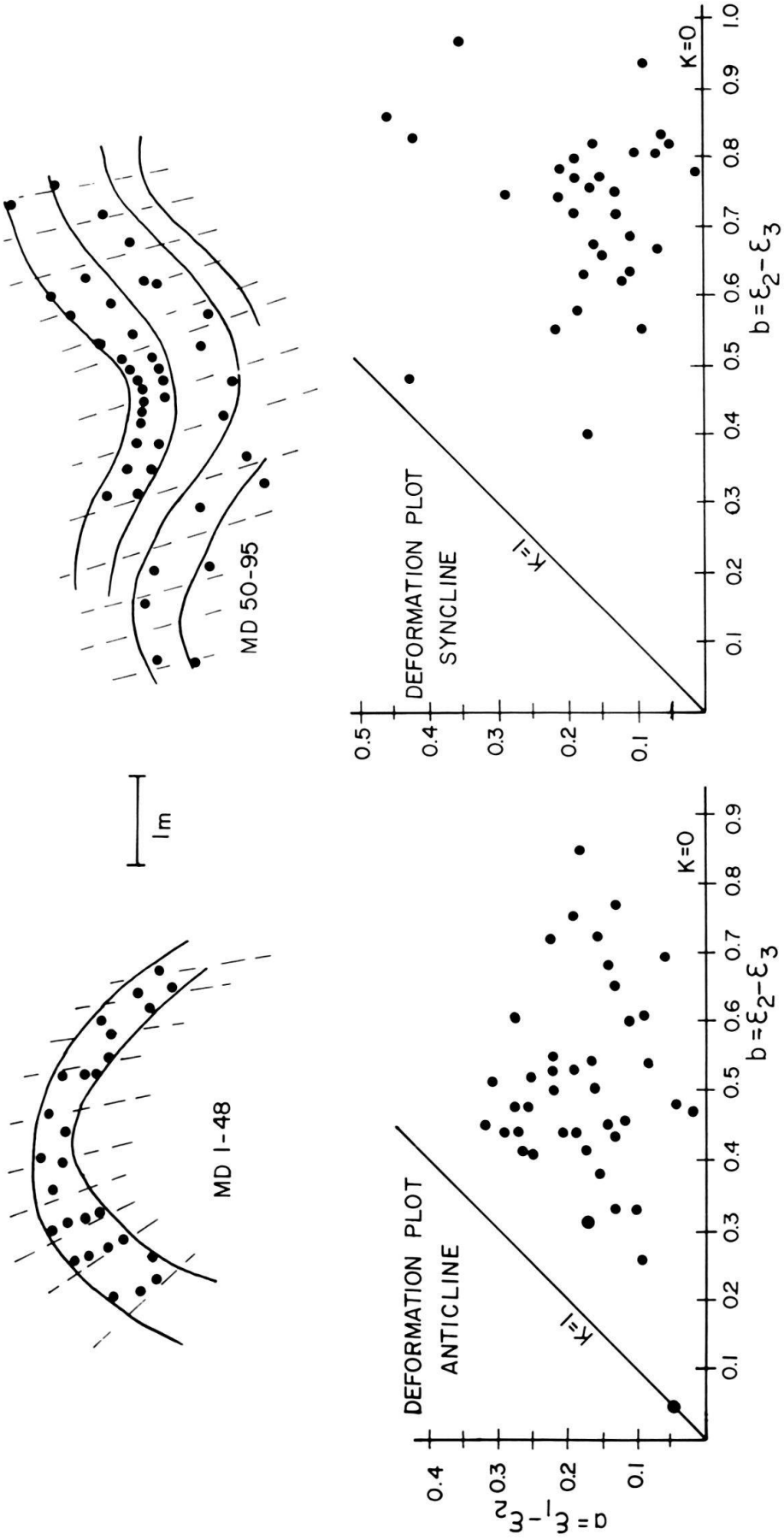

Fig. 17. Finite strains derived from magnetic susceptibility measurements at Maderanertal. The localities sampled are indicated in rough sketches (upper diagrams) and the calculated finite strains are shown on deformation plots (lower diagrams).

only two of the three normalized principal susceptibilities (and strains) are independent. As a result the regression line passes through the origin of the plot, and the correlation coefficient $r = 0.96$.

The correlation between magnetic susceptibility anisotropy and strain from the specimens shown in Figure 16 has been used to calculate the strains in the remainder of the 90 samples drilled from two folds in the Maderanertal (Fig. 17).

The finite strain results are graphically displayed on a logarithmic deformation plot (FLINN 1978, RAMSAY 1967). If $\varepsilon_i > \varepsilon_2 > \varepsilon_3$ are the principal logarithmic strains, then the ratios $a = (\varepsilon_1 - \varepsilon_2)$ and $b = (\varepsilon_2 - \varepsilon_3)$ are plotted as ordinate and abscissa respectively (Fig. 17). The data are conveniently analyzed by their location on the deformation plot in certain fields. Where K is defined such that $K = a/b$ then the deformation plot consists of the constrictional field ($\infty > K > 1$), plane strain field ($K = 1$), and flattening field ($1 > K > 0$).

In the deformation plots of Figure 17, the strain data from the anticline and the syncline lie entirely within the flattening field of the deformation plot. In both cases considerable strain variation is observed in each fold.

The large density of strain measurements obtained using this method provides an outstanding opportunity to examine the relationship of the strain variation to the geometry of the folds (RAMSAY 1967). We anticipate that the same dense network of strain results can be used together with finite element techniques to remove the strains (COBBOLD & PERCEVAULT 1981) and examine the mechanisms of fold formation in three dimensions. This is currently the subject of ongoing investigation in these rocks.

Acknowledgments

This work was financially supported by the Swiss National Science Foundation, project No. 2.859-0.77; tectonic and geophysical studies of the Helvetic Alps. We thank Dr. J.G. Ramsay for originally suggesting the project and Drs. A.G. Milnes, P. Turner, J.E.T. Channell, F. Heller and W.H. Owens for discussions at various stages of the work. Contribution Nr. 363, Institut für Geophysik, ETH-Zürich.

REFERENCES

BAKER, D.W. (1964): *Structural petrology of the Windgällen fold.* - Thesis (unpubl.), University Zürich.

BANERJEE, S.K., & STACEY, F.D. (1967): *The high-field torque meter method of measuring magnetic anisotropy of rocks.* In: COLLINSON, D.W., CREER, K.M., & RUNCORN, S.K. (Ed.): *Methods in Palaeomagnetism* (p. 470-476). - Elsevier, Amsterdam.

BARRIE, T., VAN DER VOO, R., & PEACOR, D.R. (1980): *Growth of magnetite during thermal demagnetization of Rose Hill dolomitic sandstone; optical, X-ray and rock magnetic identifications* (Abstr.) - EOS *61*, 51.

BHATHAL, R.S. (1971): *Magnetic anisotropy in rocks.* - Earth-Sci. Rev. *7*, 227-253.

BRADSHAW, M.J., JAMES, S.J., & TURNER, P. (1979): *Origin of oolitic ironstones - discussion.* - J. sediment. Petrol. *50*, 95-304.

BROOKS, P.J., & O'REILLY, W. (1970): *Magnetic rotational hysteresis characteristics of red sandstones.* - Earth and planet. Sci. Lett. *9*, 71-76.

BRÜCKNER, W. (1943): *Tektonik des oberen Schächentales (Kanton Uri).* - Beitr. geol. Karte Schweiz [N.F.] *80*, 1-42.

CLOOS, E. (1947): *Oolite deformation in the South Mountain fold, Maryland.* - Bull. geol. Soc. Amer. *58*, 843-918.

COBBOLD, P., & PERCEVAULT, M.N. (1981): *Strain removal in two and three dimensions: theory and regional applications* (Abstr.). - J. struct. Geol. *3*, 186.

DAY, R., O'REILLY, W., & BANERJEE, S.K. (1970): *Rotational hysteresis study of oxidized basalts.* - J. geophys. Res. *75*, 375-386.

DÉVERIN, L. (1945): *Etude pétrographique des minerais de fer oolithiques du Dogger des Alpes suisses.* - Beitr. Geol. Schweiz, geotech. Ser. [Liefg.] *13/2*.

DOLLFUS, S. (1965): *Über den Helvetischen Dogger zwischen Linth und Rhein.* - Eclogae geol. Helv. *58*, 453-554.

DUNLOP, D.J. (1972): *Magnetic mineralogy of unheated and heated red sediments by coercivity spectrum analysis.* - Geophys. J. r. astron. Soc. *27*, 37-55.

DUNNET, D. (1969): *A technique of finite strain analysis using elliptical particles.* - Tectonophysics *7*, 117-136.

DURNEY, D.W., & RAMSAY, J.G. (1973): *Incremental strains measured by syntectonic crystal growths.* In: DEJONG, K.A., & SCHOLTEN, R. (Ed.): *Gravity and Tectonics* (p.67-96). - J. Wiley & Sons, New York.

FLINN, D. (1978): *Construction and use of three-dimensional progressive deformations.* - J. geol. Soc. (London) *135*, 291-305.

FREY, M. (1978): *Progressive low-grade metamorphism of a black shale formation, Central Swiss Alps, with special references to pyrophyllite and margarite bearing assemblages.* - J. Petrol. *19*, 93-135.

FÜCHTBAUER, H., & MÜLLER, G. (1970): *Sedimente und Sedimentgesteine;* Teil II: *Sediment-Petrologie.* - Schweizerbart, Stuttgart.

GRAHAM, J.W. (1954): *Magnetic susceptibility anisotropy, an unexploited petrofabric element.* - Bull. geol. Soc. Amer. *65*, 1257-1258.

— (1966): *Significance of magnetic anisotropy in Appalachian sedimentary rocks.* In: STEINHART, J.S., & SMITH, T.J. (Ed.): *The Earth Beneath the Continents* (p.627-648). - Geophys. Monogr. *10*, Amer. geophys. Union, Washington D.C.

HAMILTON, N. (1963): *Susceptibility anisotropy measurements on some Silurian siltstones.* - Nature *197*, 170-171.

HAMILTON, N., & REES, A.I. (1970): *Magnetic fabric of sediments from the shelf at La Jolla (California).* - Marine Geol. *9*, 6-11.

HEIM, ALB. (1878): *Untersuchung über den Mechanismus der Gebirgsbildung im Anschluss an die Geologische Monographie der Tödi-Windgällen-Gruppe* (Bd.I/II + Atlas). - Schwabe, Basel.

— (1919): *Geologie der Schweiz* (Bd.II/1). - Tauchnitz, Leipzig.

HEIM, ALB., & HEIM, ARN. (1916): *Die Juramulde im Aarmassiv bei Fernigen (Uri).* - Vjschr. natf. Ges. Zürich *61*, 503-530.

HEINIGER, C., & HELLER, F. (1976): *A high temperature vector magnetometer.* - Geophys. J. r. astron. Soc. *44*, 281-288.

HELLER, F. (1973): *Magnetic anisotropy of granitic rocks of the Bergell Massif (Switzerland).* - Earth and planet. Sci. Lett. *20*, 180-188.

HENRY, B. (1973): *Studies of microtectonics, anisotropy of magnetic susceptibility, and palaeomagnetism of the Permian Dome de Barrot (France): paleotectonic and paleosedimentological implications.* - Tectonophysics *17*, 61-72.

HROUDA, F. (1976): *A model for the orientation process of ferromagnetic minerals in slates.* - Earth and planet. Sci. Lett. *33*, 107-110.

— (1978): *The magnetic fabric in some folds.* - Phys. earth planet. interiors *17*, 89-97.

— (1979): *The strain interpretation of magnetic anisotropy in rocks of the Nizky Jesenik mountains (Czechoslovakia).* - Sb. geol. Věd, Uzita Geofyz. *16*, 27-62.

HROUDA, F., & JANAK, F. (1971): *A study of the hematite fabric of some red sediments on the basis of their magnetic susceptibility anisotropy.* - Sediment. Geol. *6*, 187-199.

— (1976): *The changes in shape of the magnetic susceptibility ellipsoid during progressive metamorphism and deformation.* - Tectonophysics *34*, 135-148.

KENT, D.V., & LOWRIE, W. (1975): *On the magnetic susceptibility anisotropy of deep sea sediment.* - Earth and planet. Sci. Lett. *28*, 1-12.

KIMBERLEY, M.M. (1979): *Origin of oolitic iron formations.* - J. sediment. Petrol. *49*, 111-132.

KLIGFIELD, R., LOWRIE, W., & DALZIEL, I.W.D. (1977): *Magnetic susceptibility anisotropy as a strain indicator in the Sudbury Basin, Ontario.* - Tectonophysics *40*, 287-305.

KLIGFIELD, R., OWENS, W.H., & LOWRIE, W. (1981): *Magnetic susceptibility anisotropy, strain and progressive deformation in Permian sediments from the Maritime Alps (France).* - Earth and planet. Sci. Lett. *55*, 181-189.

KNEEN, S.J. (1976): *The relationship between the magnetic and strain fabrics of some hematite bearing slates.* - Earth and planet. Sci. Lett. *31*, 413-416.

MANSON, A.J., O'DONOVAN, J.B., & O'REILLY, W. (1979): *Magnetic rotational hysteresis loss in titanomagnetites and titanomaghemites - application to non-destructive mineral identification in basalts.* - J. Geophys. *46*, 185-199.

MILNES, A.G., & PFIFFNER, O.A. (1977): *Structural development of the Infrahelvetic complex, eastern Switzerland.* - Eclogae geol. Helv. *70*, 83-95.

— (1980): *Tectonic evolution of the Central Alps in the cross section St. Gallen-Como.* - Eclogae geol. Helv. *73*, 619-633.

MÜLLER, F. (1938): *Geologie der Engelhörner, der Aareschlucht und der Kalkkeile bei Innertkirchen.* - Beitr. geol. Karte Schweiz [N.F.] *74*.

NAGATA, T., KOBAYASHI, K., & FULLER, M. (1964): *Identification of magnetite and hematite in rocks by magnetic observation at low temperatures.* - J. geophys. Res. *69*, 2111-2120.

OSBORN, J.A. (1945): *Demagnetizing factors of the general ellipsoid.* - Phys. Rev. *67*, 351-357.

OWENS, W.H. (1974): *Mathematical model studies on factors affecting the magnetic anisotropy of deformed rocks.* - Tectonophysics *24*, 115-131.

OWENS, W.H., & BAMFORD, D. (1976): *Magnetic, seismic, and other anisotropic properties of rock fabrics.* - Phil. Trans. r. Soc. London (A) *283*, 55-68.

OWENS, W.H., & RUTTER, E. (1978): *The development of magnetic susceptibility anisotropy through crystallographic preferred orientation in a calcite rock.* - Phys. earth planet. interiors *16*, 215-222.

PARRY, G.R. (1971): *The magnetic anisotropy of some deformed rocks.* - Ph.D. Thesis (unpubl.), University Birmingham.

PFIFFNER, O.A. (1977): *Tektonische Untersuchungen im Infrahelvetikum der Ostschweiz.* - Mitt. geol. Inst. ETH u. Univ. Zürich [N.F.] *217*.

— (1978): *Der Falten- und Kleindeckenbau im Infrahelvetikum der Ostschweiz.* - Eclogae geol. Helv. *71*, 61-84.

— (1980): *Strain analysis in folds (Infrahelvetic complex, Central Alps).* - Tectonophysics *61*, 337-362.

— (1981a): *Substructures and microstructures in naturally deformed limestones (Helvetic zone, E. Switzerland).* - Habil. thesis (unpubl.), University Neuchâtel.

— (1981b): *Fold- and- thrust tectonics in the Helvetic nappes (E. Switzerland).* In: MCCLAY, K.R., & PRICE, N.J. (Ed.): *Thrust and Nappe Tectonics* (p.319-327). - Spec. Publ. geol. Soc. London *9*.

PORATH, H., & CHAMALAUN, F.H. (1966): *The magnetic anisotropy of hematite bearing rocks.* - Pure and appl. Geophys. *64*, 81-88.

RAMSAY, J.G. (1967): *Folding and Fracturing of Rocks.* - McGraw Hill, New York.

RATHORE, J.S. (1979): *Magnetic susceptibility anisotropy in the Cambrian slate belt of North Wales and correlation with strain.* - Tectonophysics *24*, 115-136.

REES, A.I. (1965): *The use of anisotropy of magnetic susceptibility in the estimation of sedimentary fabric.* - Sedimentology *4*, 257-271.

ROBIN, P. (1977): *Determination of geologic strain using randomly oriented strain markers of any shape.* - Tectonophysics *42*, T7-T16.

SCHWARZ, E.J., & HARRIS, D.C. (1970): *Phases in natural pyrrhotite and the effect of heating on their magnetic properties and compositions.* - J. Geomagn. Geoelectr. *22*, 463-470.

SCRIBA, H., & HELLER, F. (1978): *Measurements of anisotropy of magnetic susceptibility using inductive magnetometers.* - J. Geophys. *44*, 341-352.

SIDDANS, A.W.B. (1971): *The origin of slaty cleavage.* - Ph.D. thesis (unpubl.), University London.

— (1980): *Analysis of three dimensional, homogeneous finite strain using ellipsoidal objects.* - Tectonophysics *64*, 1-16.

SPÖRLI, B.K. (1966): *Geologie der östlichen und westlichen Urirotstock-Gruppe.* - Mitt. geol. Inst. ETH u. Univ. Zürich [N.F.] *62*.

STACEY, F. (1963): *The physical theory of rock magnetism.* - Adv. Phys. *12*, 45-133.

STONER, E.C. (1945): *The demagnetizing factor for ellipsoids.* - Phil. Mag. *36*, 803.

TAN, B.K. (1969): *Analysis of tectonic strain in Windgällen and Färnigen, Canton Uri, Switzerland.* - Ph.D. thesis (unpubl.), Imperial College, London.

— (1976): *Oolite deformation in Windgällen, Canton Uri, Switzerland.* - Tectonophysics *31*, 157-174.

UYEDA, S., FULLER, M.D., BELSHE, J.C., & GIRDLER, R.W. (1963): *Anisotropy of magnetic susceptibility of rocks and minerals.* - J. geophys. Res. *68*, 279-291.

VAN DEN ENDE, C. (1977): *Paleomagnetism of Permian red beds of the Dome de Barrot (S. France).* - Ph.D. thesis (unpubl.), University Utrecht.

WOOD, D.S., OERTEL, G., SINGH, J., & BENNETT, H.F. (1976): *Strain and anisotropy in rocks.* - Phil. Trans r. Soc. London (A) *283*, 27-42.